



UNIVERSITÀ
DI TORINO



Functional characterization and functionalization of materials by ion beams.

Ettore Vittone

Physics Department

University of Torino (I)

Functional characterization of semiconductor materials and devices

Measurement of the their electronic properties and performances

Main physical observable: current

Current = F(carrier density; carrier transport)

Carrier (electron-hole) generation
Recombination/trapping

Carrier lifetime τ

Free carriers (electron/hole) transport
Two mechanisms:

Drift \Rightarrow electric field $\mathbf{v} = \mu \cdot \mathbf{E}$

Diffusion \Rightarrow concentration gradient

NIMB 93 (1979) 160, 73

**ELECTRICAL PROPERTIES AND PERFORMANCES
OF NATURAL DIAMOND NUCLEAR RADIATION DETECTORS**

C. CANALI¹, E. GATTI², S. F. KOZLOV⁴, P. F. MANFREDI³,
C. MANFREDOTTI⁵, F. NAVA¹, and A. QUIRINI⁵

¹ Institute of Physics, University of Modena, Modena, Italy

² Institute of Physics, Politecnico di Milano and INFN Milano, Milan, Italy

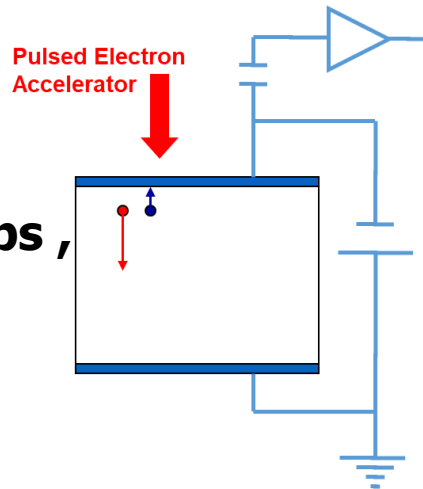
³ Cesnef, Politecnico di Milano and INFN Milano, Milan, Italy

⁴ Institute of Physics Lebedev, Academy of Sciences of U.S.S.R., Moscow, U.S.S.R.

⁵ Institute of Physics, University of Bari, Bari, Italy

**40 keV pulsed
electron
accelerator, 70 ps ,**

**RevScInstr 41,
1205 (1970)**



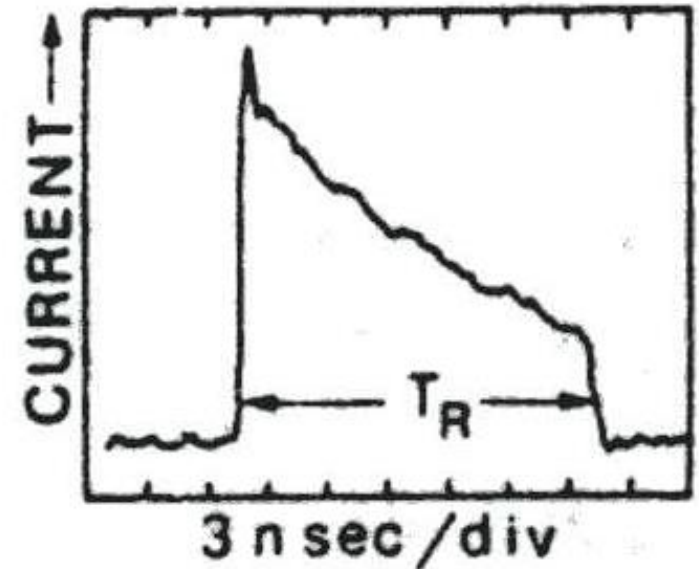
Natural IIa diamond from Yakutia (Siberia USSR)

400 μm thick

$\rho \approx 10^{15} \Omega \cdot \text{cm}$; $\epsilon = 0.5 \text{ pF/cm}$;

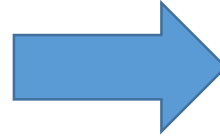
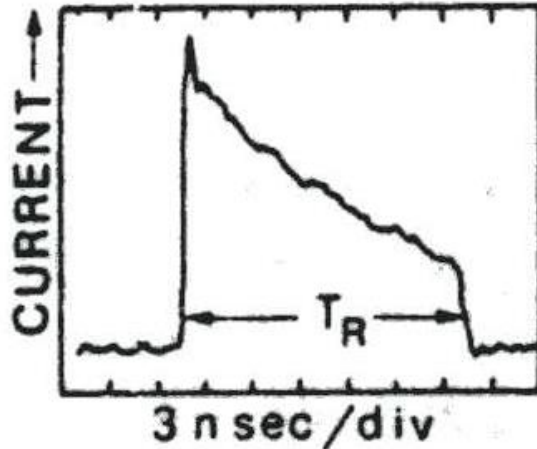
Dielectric relaxation time = 500 s.

Charge neutrality not maintained

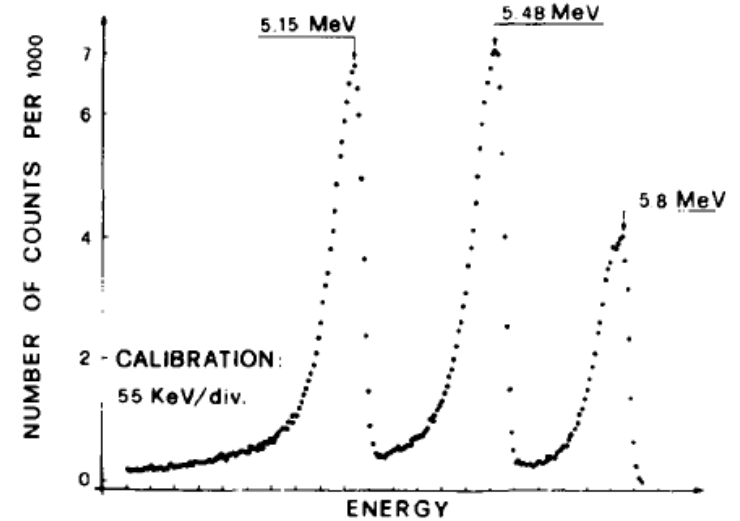


**$T_R \rightarrow$ drift velocity \rightarrow mobility
Current decay \rightarrow carrier lifetime**

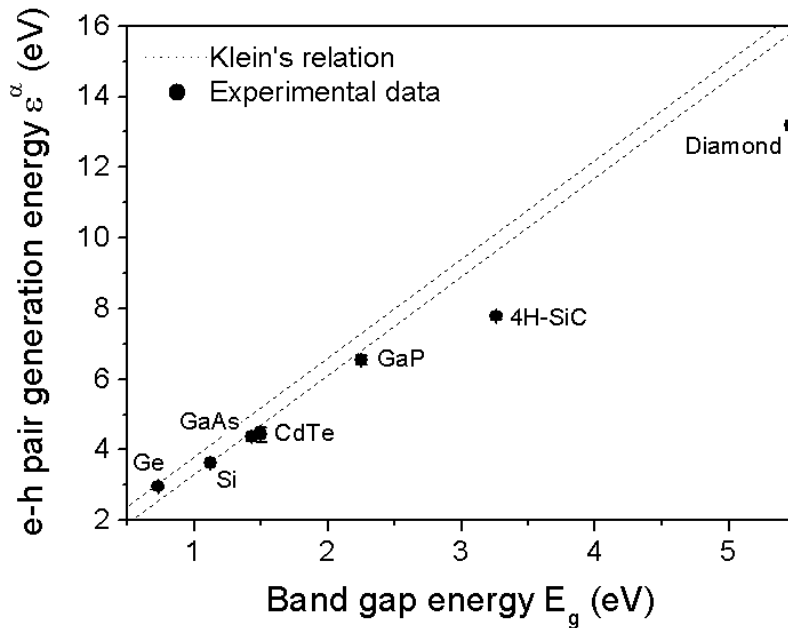
Electron beam induced current



Ion beam induced charge



Alpha spectra from a source containing a mixture of ^{231}Am , ^{239}Pu and ^{244}Cm .

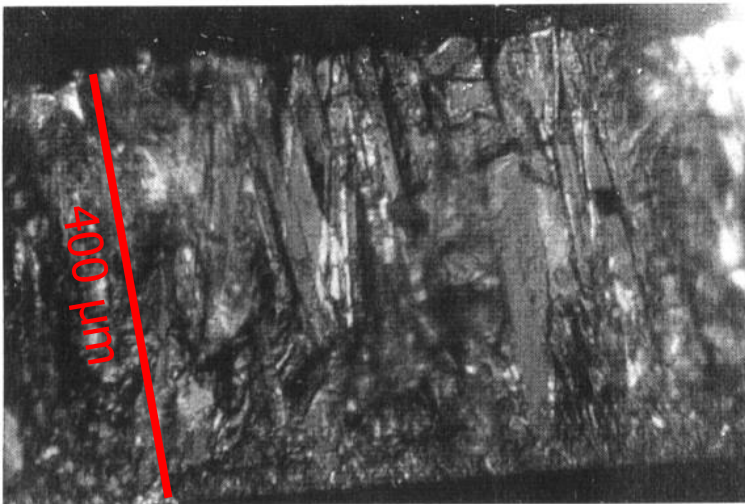
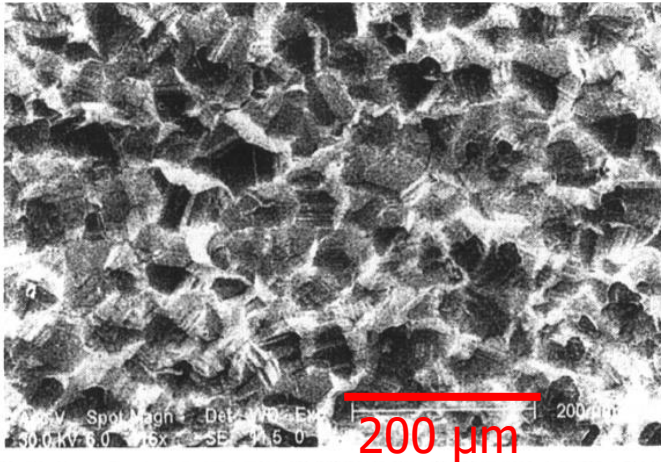


$$N_{eh} = \frac{E_{ion}}{\epsilon_{eh}}$$

**1 MeV alpha in
Diamond generates
about 78000 e/h pairs**



**Single ion
detection**

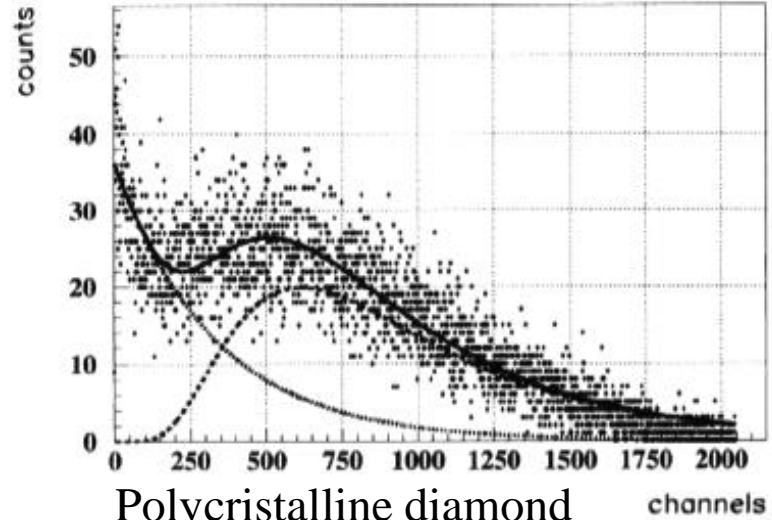


microscope image showing the first 200 μm of thickness of a CVD diamond sample from the

Grain size effects in CVD diamond detectors

C. Manfredotti *, F. Fizzotti, E. Vittone, S. Bistolfi, M. Boero, P. Polesello

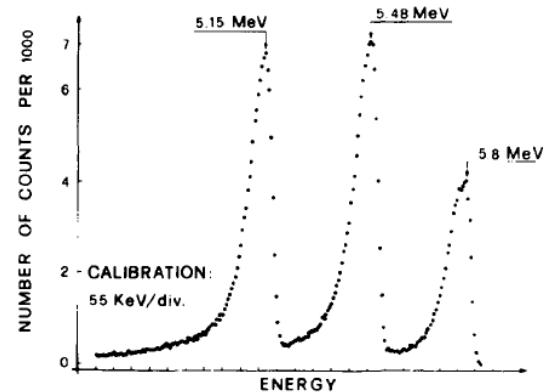
Experimental Physics Dept., University of Torino, Via Giuria 1, Torino, Italy and National Institute for Nuclear Physics (INFN), Sez. of Torino, Italy



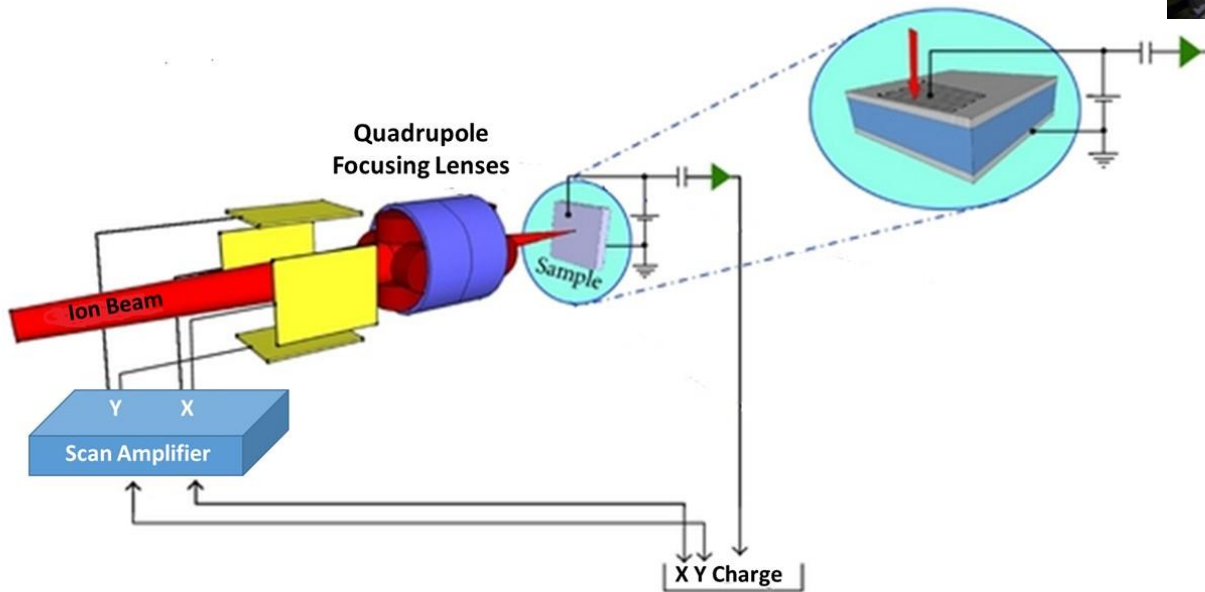
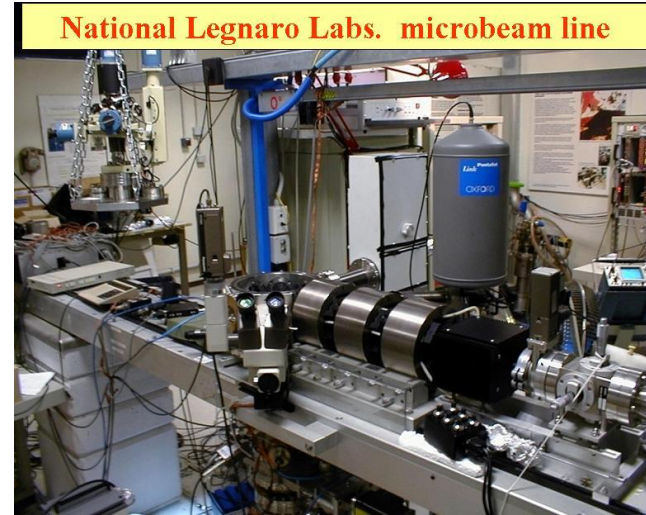
Polycrystalline diamond

Alpha particle spectrum

Monocrystalline diamond



Ion Beam Induced Charge IBIC

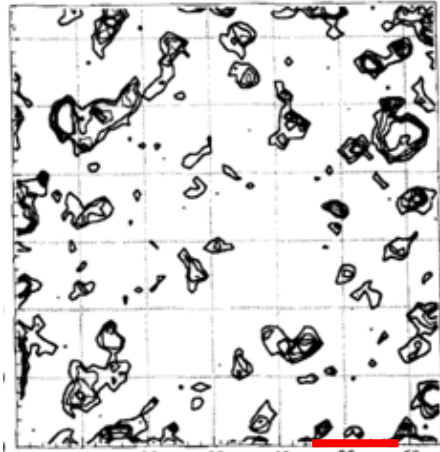


**Nuclear microprobe facility
@ Ruđer Bošković Institute
(Zagreb, Croatia)**

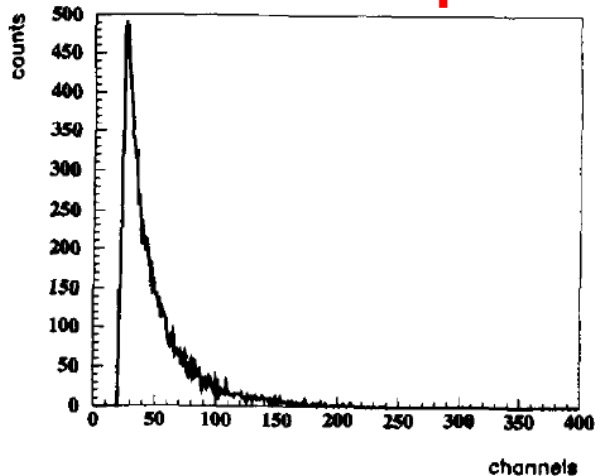


IBIC investigations on CVD diamond

UNIVERSITÀ DEGLI STUDI DI TORINO
 DI C. Manfredotti ^{a,b,*}, F. Fizzotti ^{a,b}, E. Vittone ^{a,b}, M. Boero ^{a,b}, P. Polesello ^a,
 S. Galassini ^{c,d}, M. Jaksic ^e, S. Fazinic ^e, I. Bogdanovic ^e

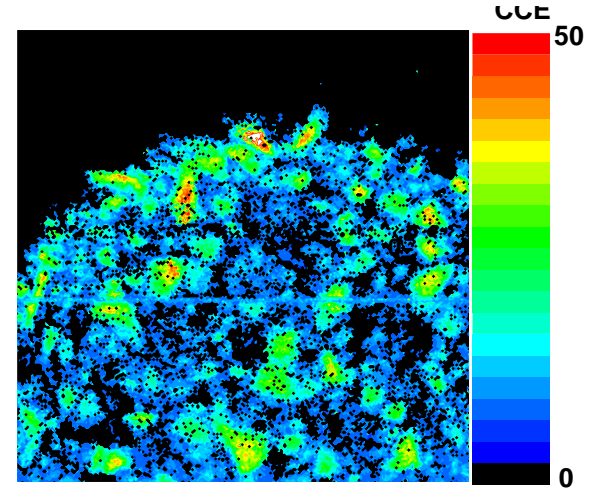


100 μm

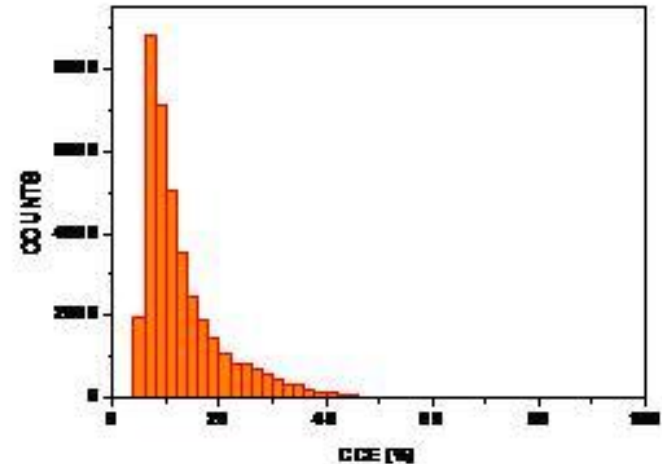


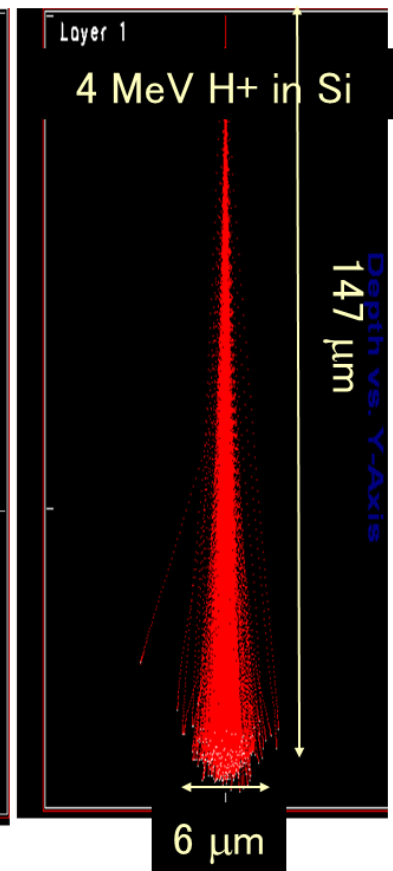
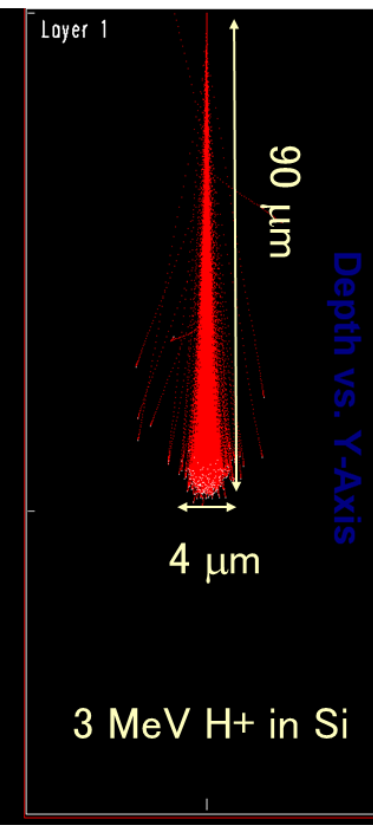
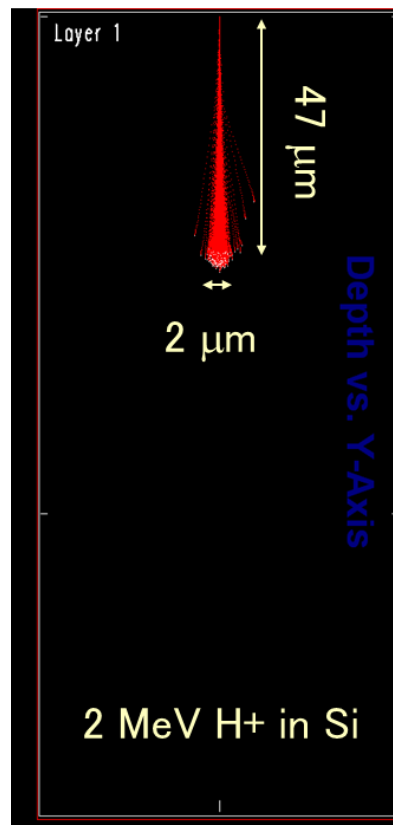
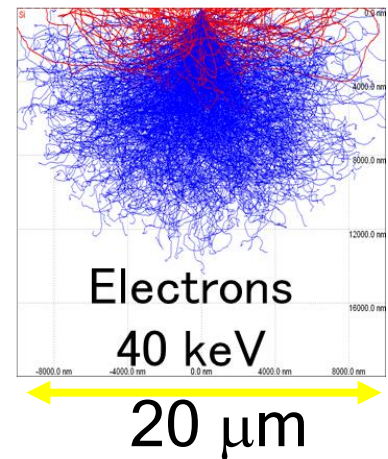
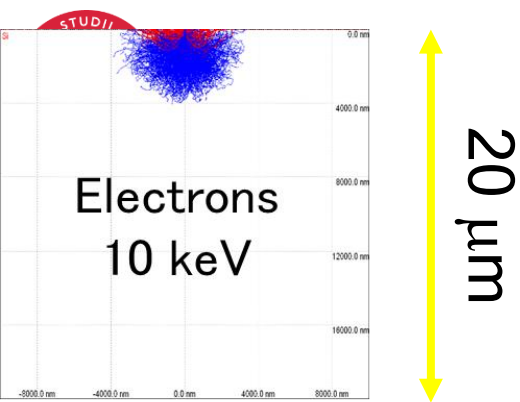
Blue light sensitization of CVD diamond detectors

C. Manfredotti^{a,b,*}, E. Vittone^{a,b}, C. Paolini^{a,b}, P. Olivero^{a,b}, A. Lo Giudice^b



300 μm





With respect to OBIC, XBIC, EBIC

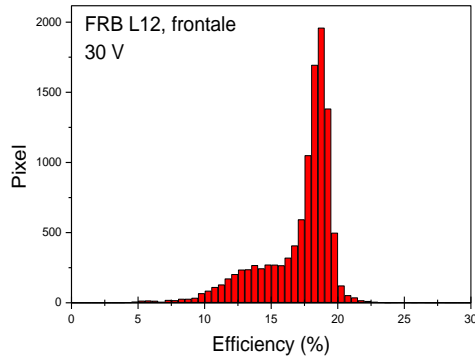
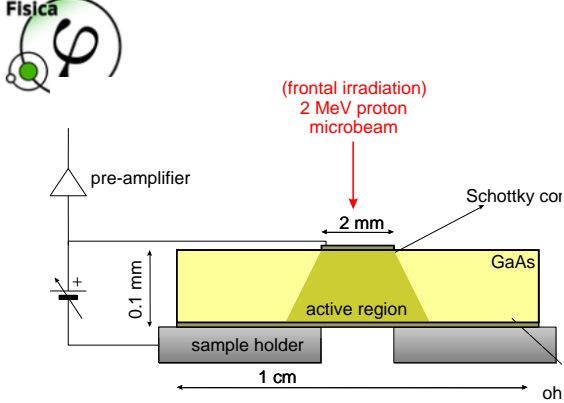
- larger analytical depth
- lower scattering through the surface layers
- flexibility due to the possibility of using ions with different mass and energy



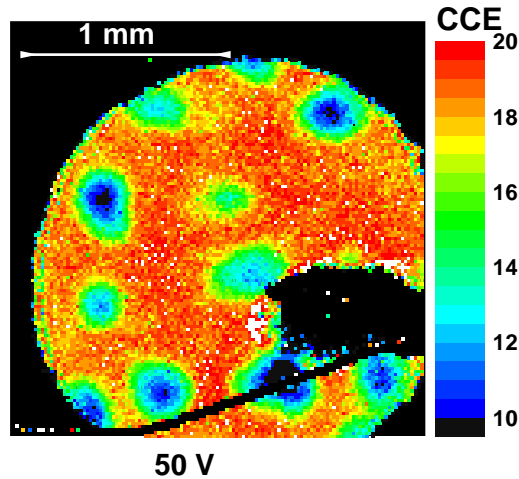
Higher spatial resolution
in buried layers
Depth profiling

IBIC analysis of gallium arsenide Schottky diodes

E. Vittone^{a,b,*}, F. Fizzotti^{a,b}, K. Mirri^a, E. Gargioni^{a,b}, P. Polesello^{a,b},
A. LoGiudice^{a,b}, C. Manfredotti^{a,b}, S. Galassini^c, P. Rossi^d, P. Vanni^e, F. Nava^e

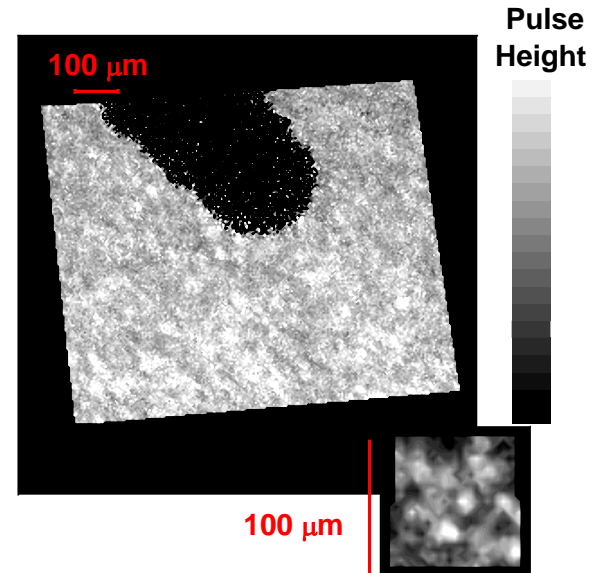
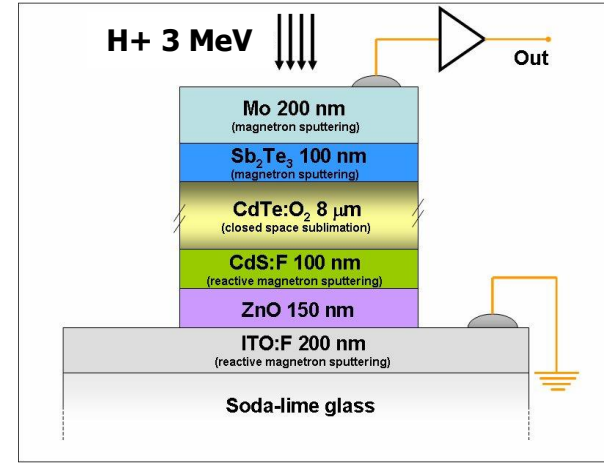


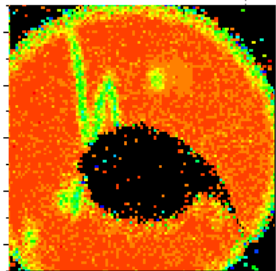
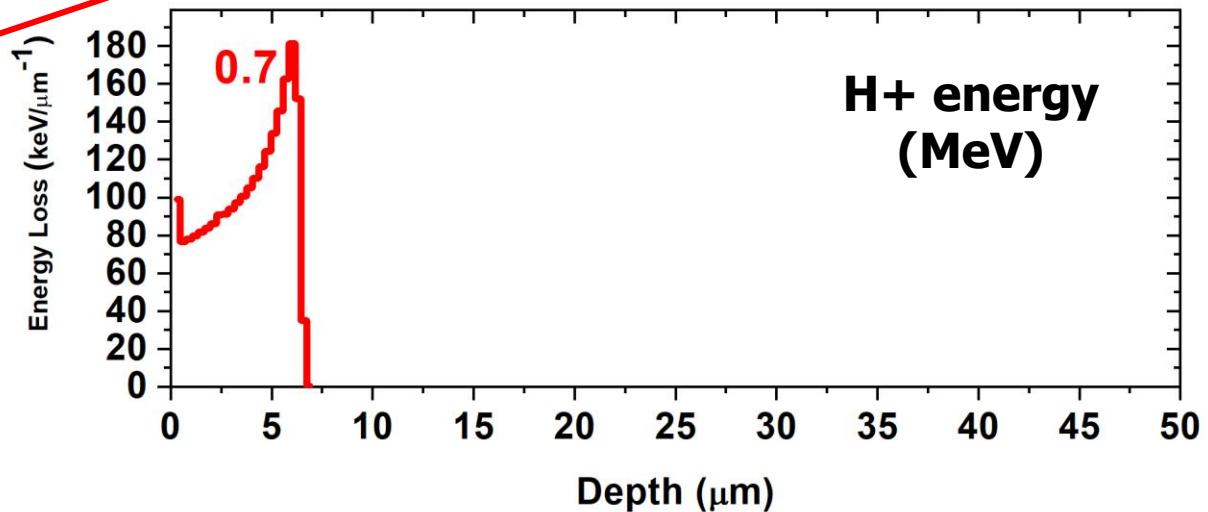
the material behaves as a "mixture" of two "electronic phases"

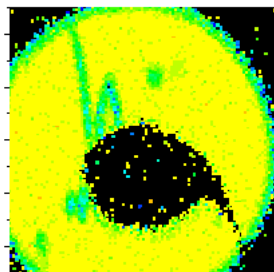
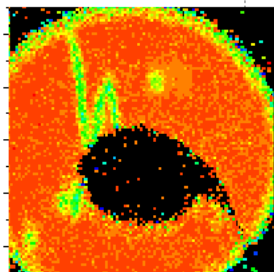
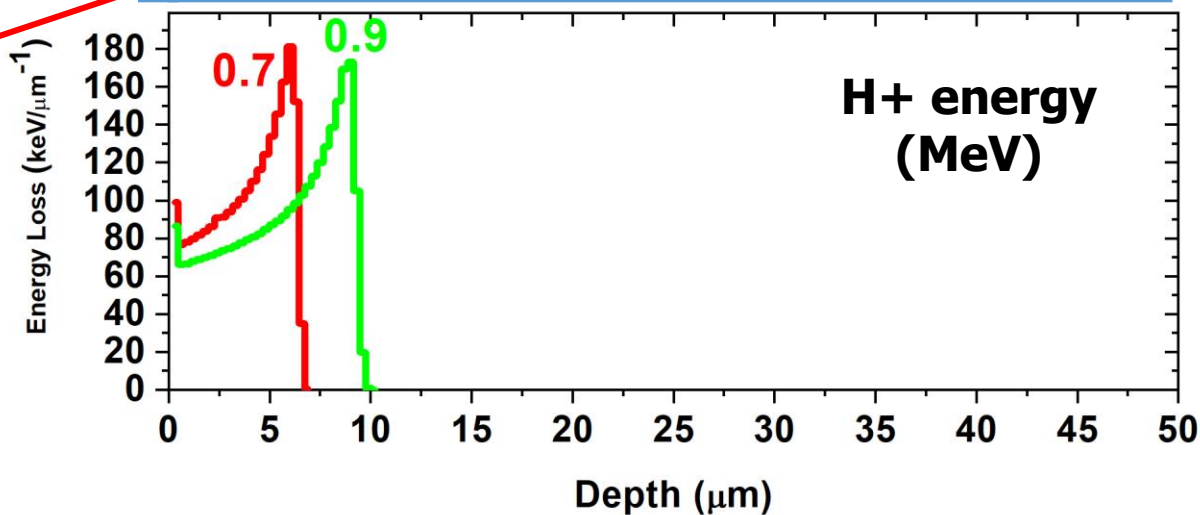


IBIC analysis of CdTe/CdS solar cells

E. Colombo^{a,b}, A. Bosio^c, S. Calusi^{a,d}, L. Giuntini^d, A. Lo Giudice^{a,b}, C. Manfredotti^{a,b},
M. Massi^d, P. Olivero^{a,b}, A. Romeo^e, N. Romeo^c, E. Vittone^{a,b,*}



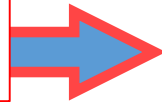
**Frontal ion
Irradiation****Schottky
electrode****50 μm thick N-type epitaxial 4H-SiC layer****Depletion
region****1 mm**

**Frontal ion
Irradiation****Schottky
electrode****50 μm thick N-type epitaxial 4H-SiC layer****Depletion
region****1 mm****CCE**

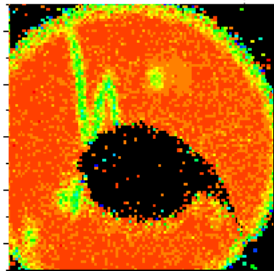
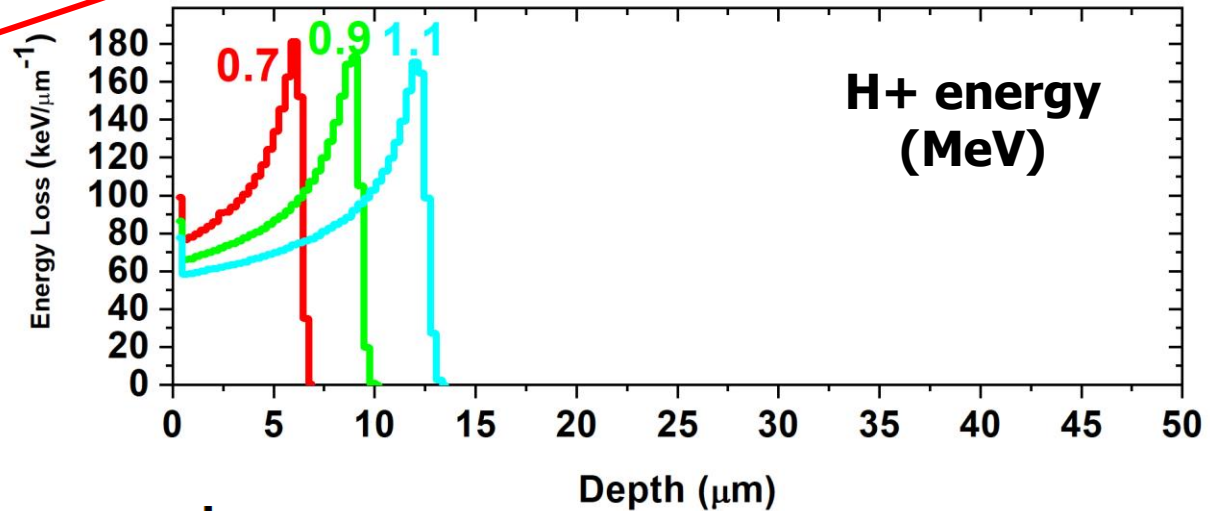
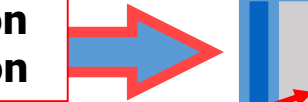
Schottky
electrode

50 μm thick N-type epitaxial 4H-SiC layer

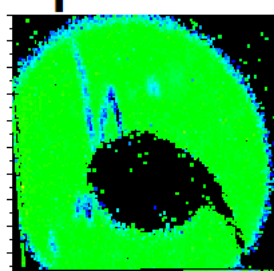
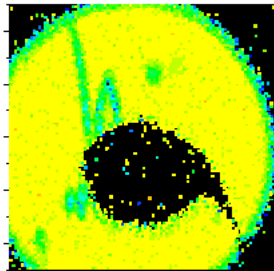
Frontal ion
Irradiation



Depletion
region



1 mm



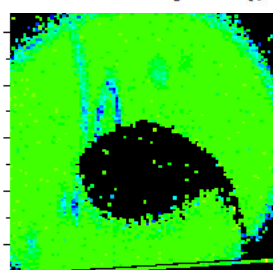
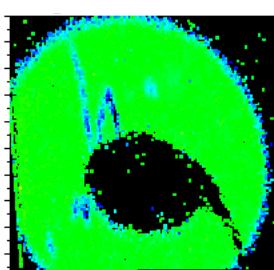
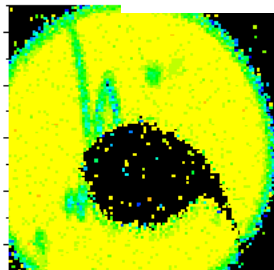
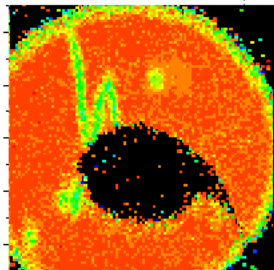
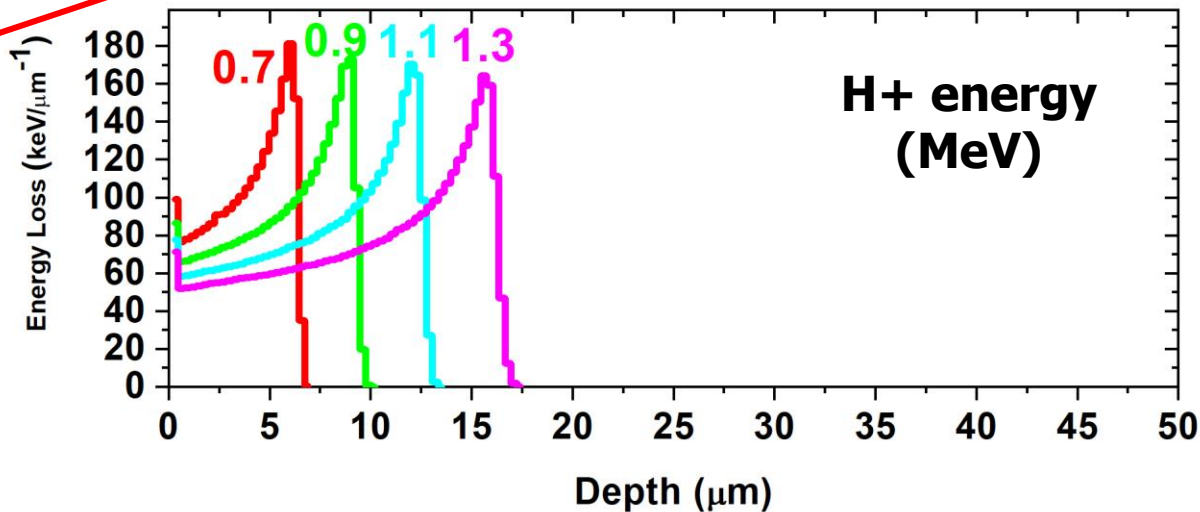


Schottky electrode

50 μm thick N-type epitaxial 4H-SiC layer

Frontal ion Irradiation

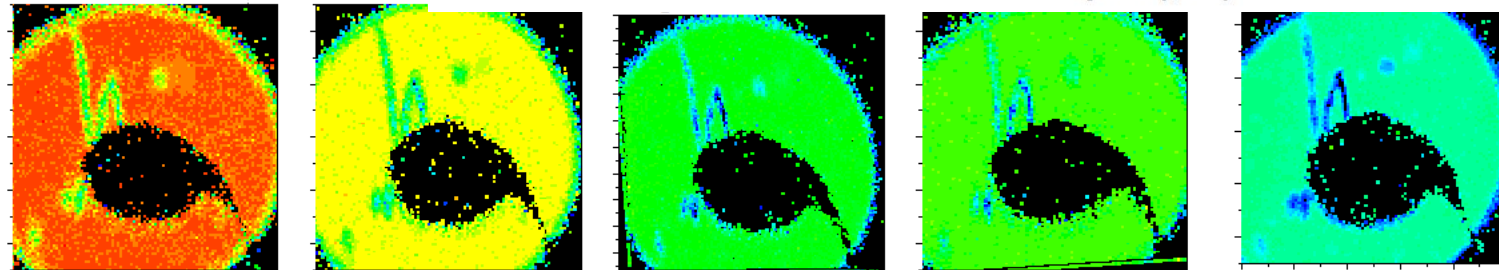
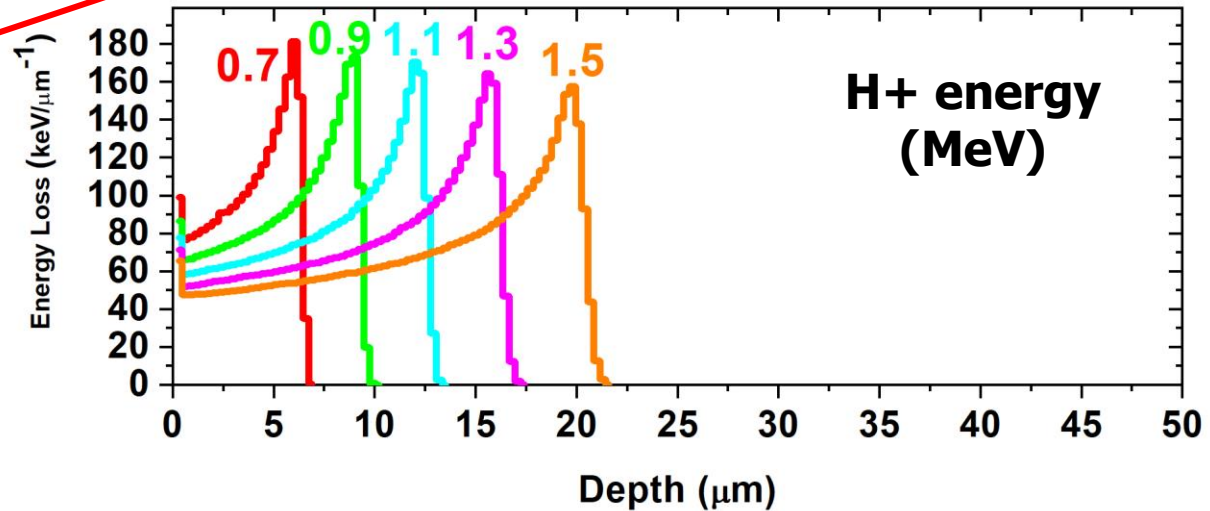
Depletion region



1 mm

CCE



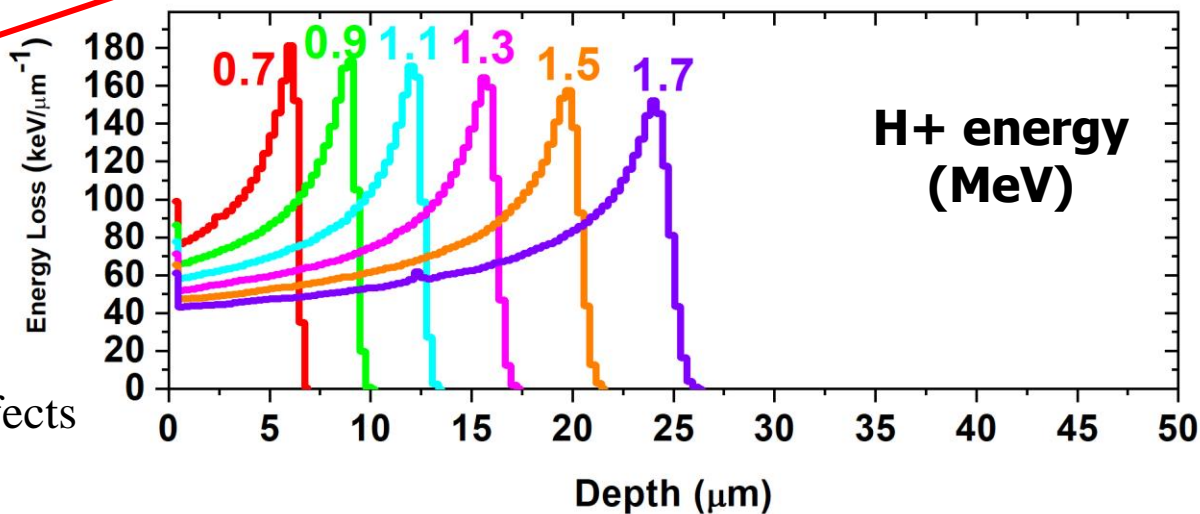
**Schottky
electrode****50 μm thick N-type epitaxial 4H-SiC layer****Frontal ion
Irradiation****Depletion
region****CCE**

**Frontal ion
Irradiation**

**Schottky
electrode**

50 μm thick N-type epitaxial 4H-SiC layer

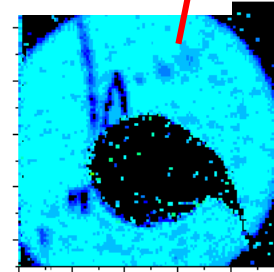
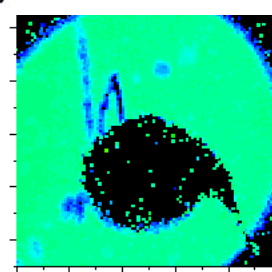
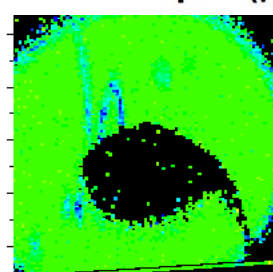
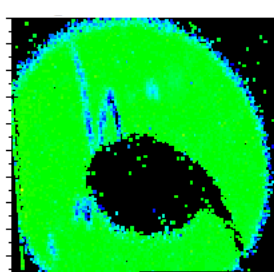
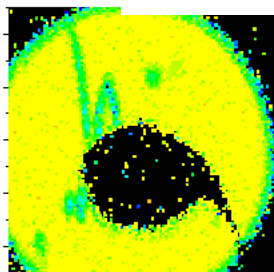
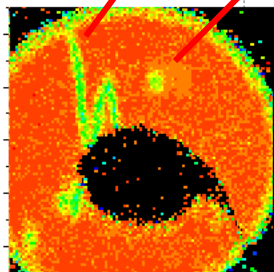
**Depletion
region**



Scratch

Surface defects

Bulk defects



1 mm

CCE





4H-SiC Schottky diode

Starting Material: 360 μm n-type 4H-SiC by CREE (USA)

Epitaxial layer from Institute of Crystal Growth (IKZ), Berlin, Germany

Devices from Alenia Marconi System

1.5 or 2.0

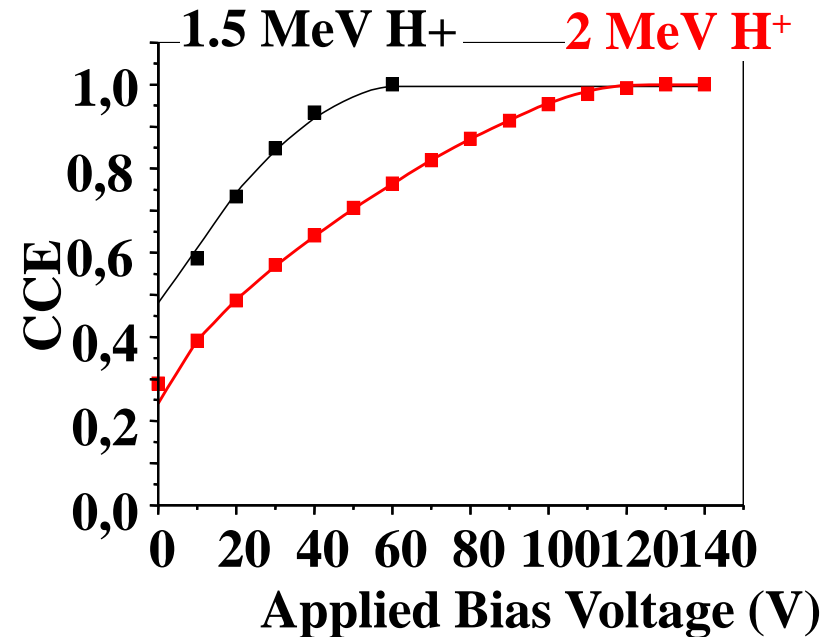
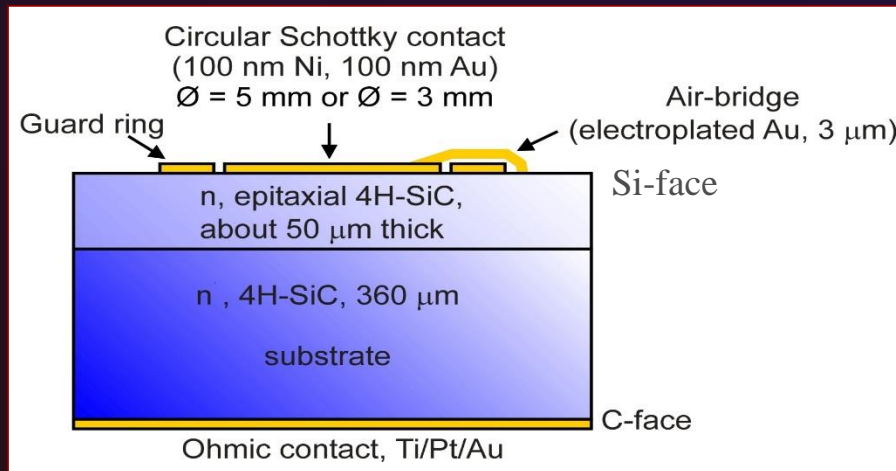
MeV H^+



CCE=Charge Collection Efficiency

=

(Charge collected)/(Charge generated)

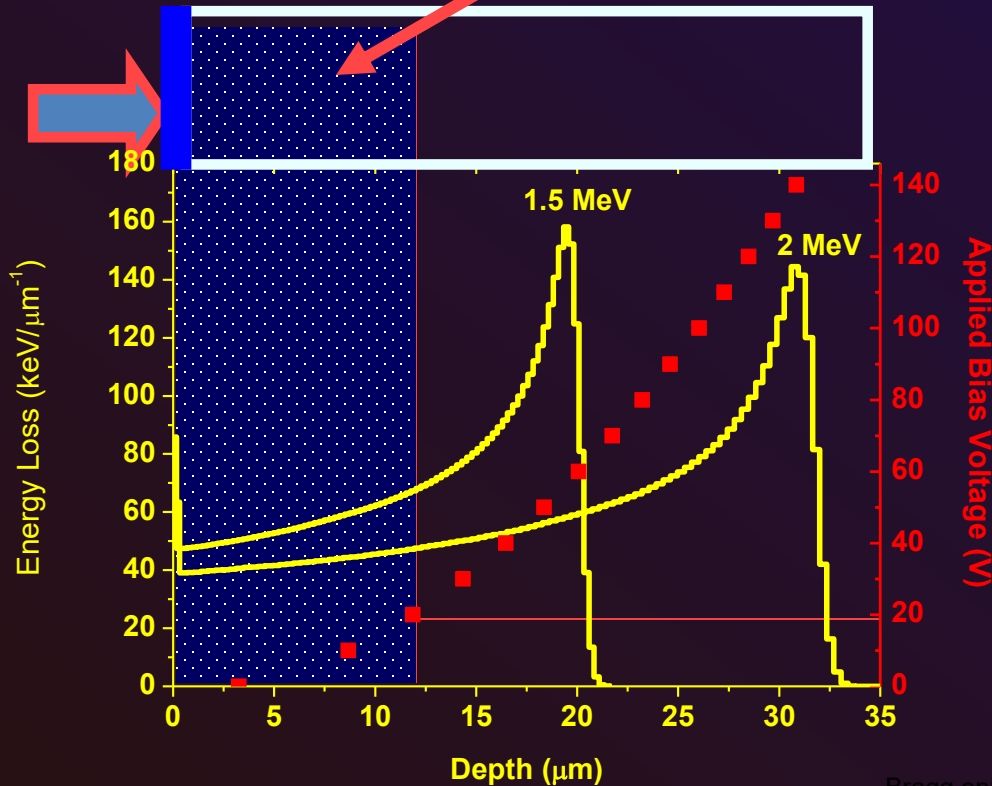


Contribution from the neutral region

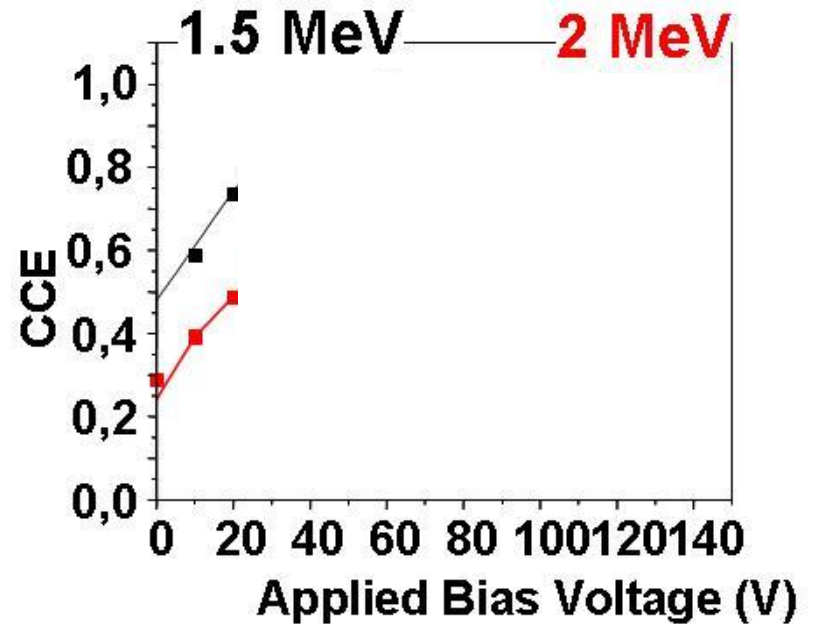
Contribution from the depletion layer

$$Q = Q_{\text{Depl}} + Q_{\text{Neutr}} \propto \left[\int_0^w \left(\frac{dE}{dx} \right) \cdot dx \right] + \left[\int_w^d \left(\frac{dE}{dx} \right) \cdot \exp \left[-\frac{x - W}{L_p} \right] \cdot dx \right]$$

Frontal ion
Irradiation



4H-SiC Schottky diode



Bragg.opj

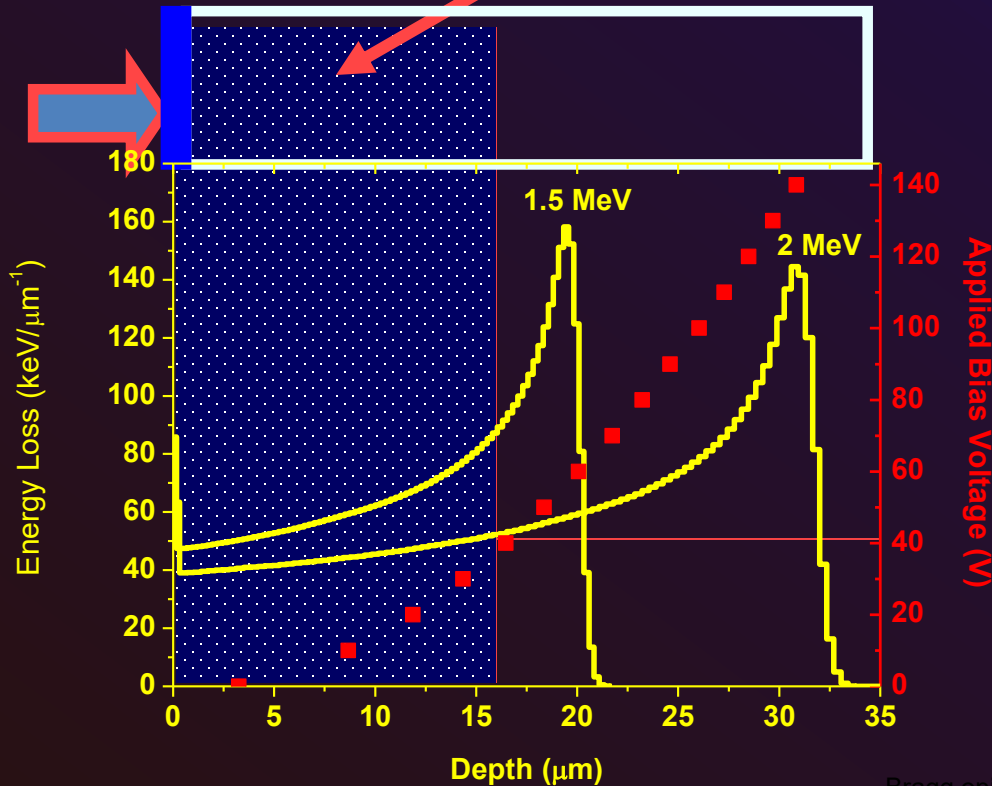


Contribution from the neutral region

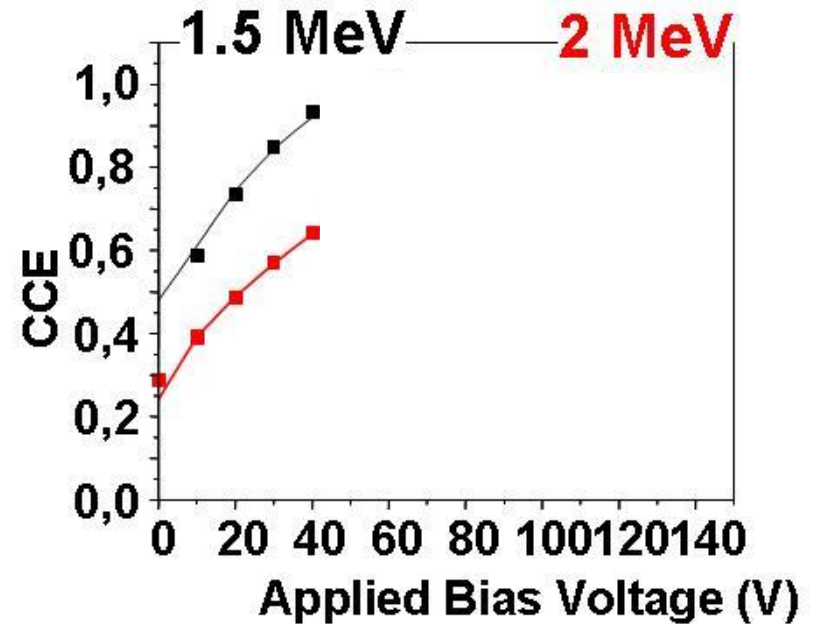
Contribution from the depletion layer

$$Q = Q_{\text{Depl}} + Q_{\text{Neutr}} \propto \left[\int_0^w \left(\frac{dE}{dx} \right) \cdot dx \right] + \left[\int_w^d \left(\frac{dE}{dx} \right) \cdot \exp \left[-\frac{x - W}{L_p} \right] \cdot dx \right]$$

Frontal ion
Irradiation



4H-SiC Schottky diode



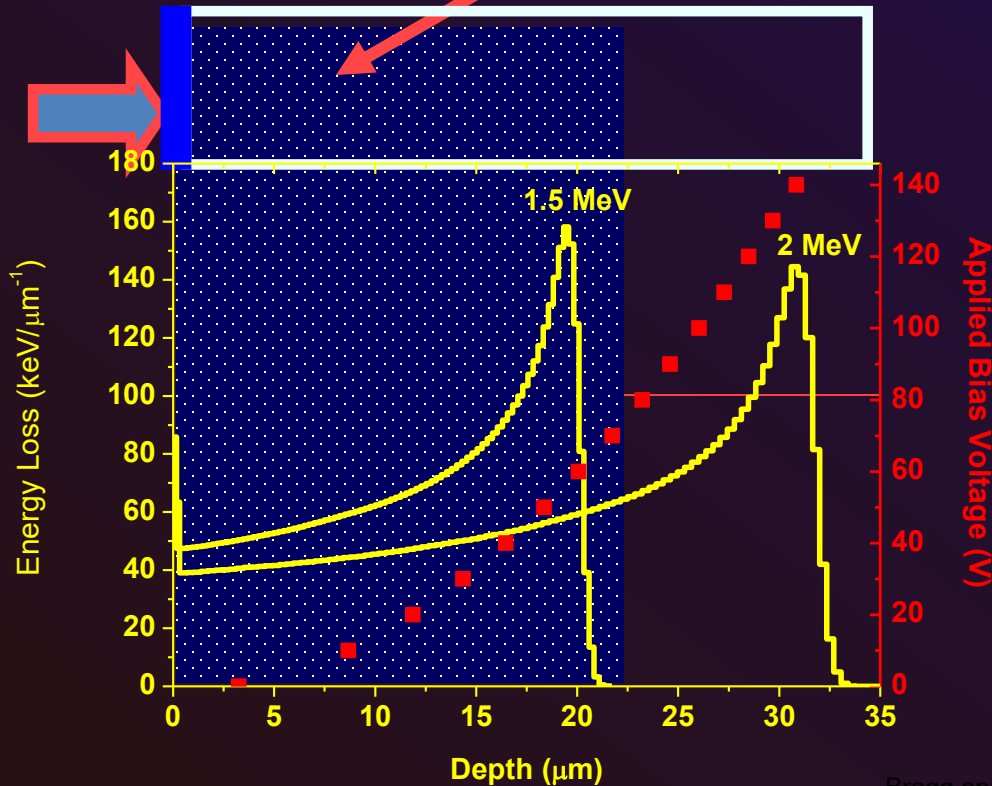
Bragg.opj



Contribution from the depletion layer

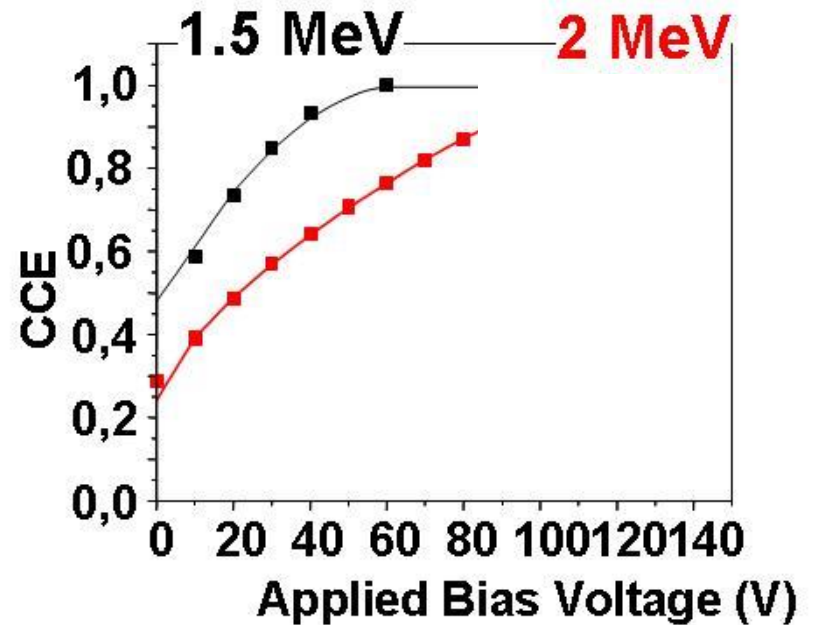
$$Q = Q_{\text{Depl}} + Q_{\text{Neutr}} \propto \left[\int_0^w \left(\frac{dE}{dx} \right) \cdot dx \right] + \left[\int_w^d \left(\frac{dE}{dx} \right) \cdot \exp \left[-\frac{x - W}{L_p} \right] \cdot dx \right]$$

Frontal ion Irradiation



Bragg.opj

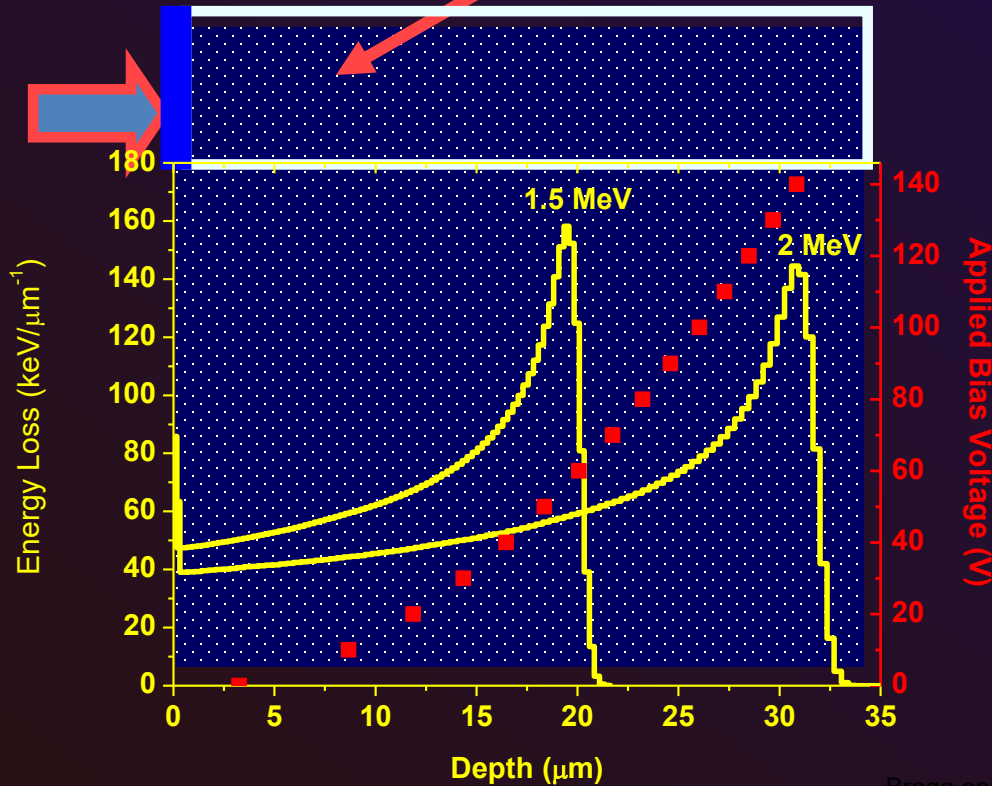
4H-SiC Schottky diode



Contribution from the depletion layer

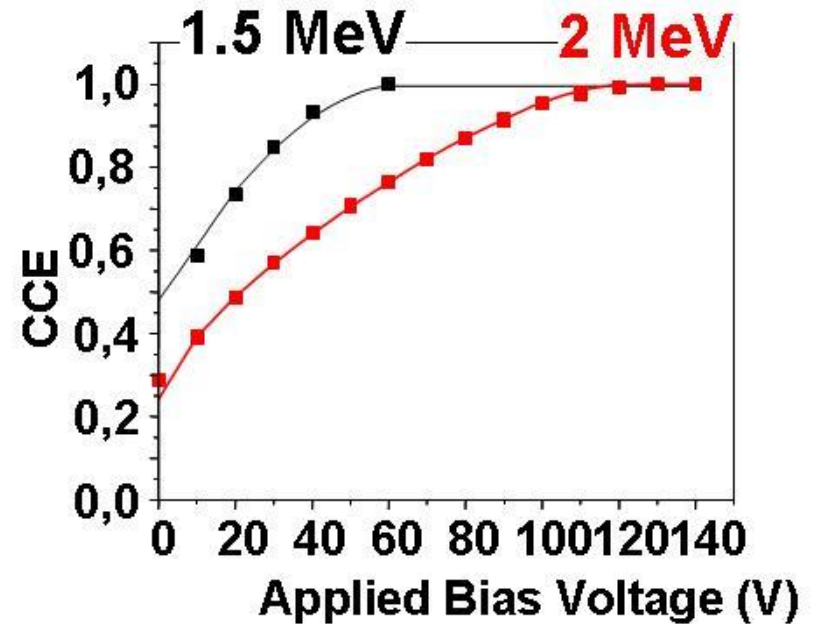
$$Q = Q_{\text{Depl}} + Q_{\text{Neutr}} \propto \left[\int_0^w \left(\frac{dE}{dx} \right) \cdot dx \right] + \left[\int_w^d \left(\frac{dE}{dx} \right) \cdot \exp \left[-\frac{x - W}{L_p} \right] \cdot dx \right]$$

Frontal ion irradiation



Bragg.opj

4H-SiC Schottky diode



Contribution from the neutral region

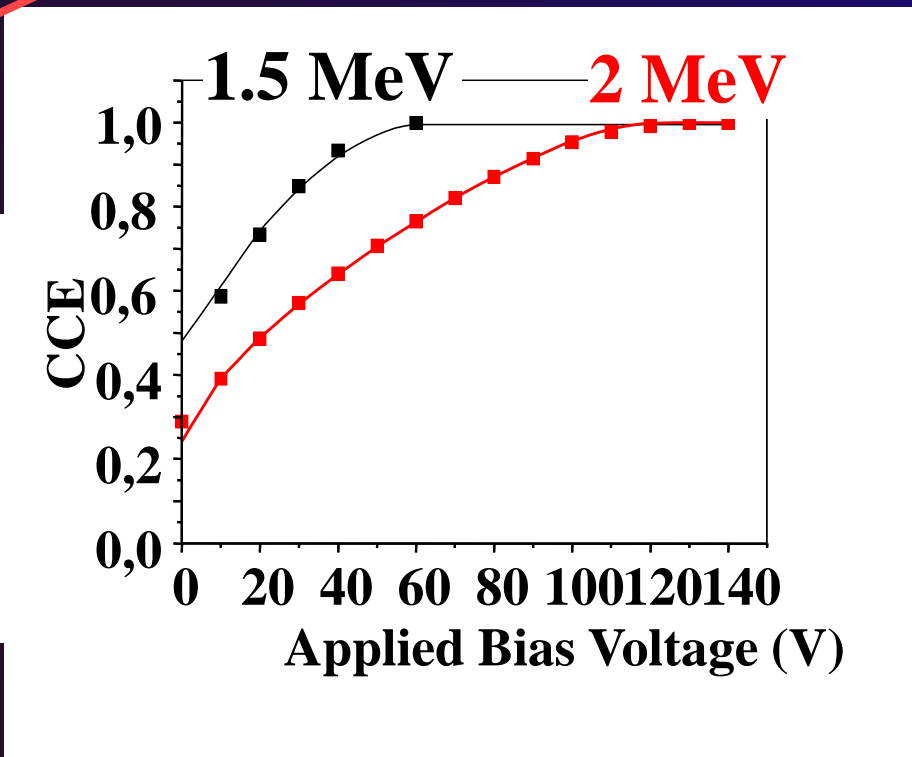
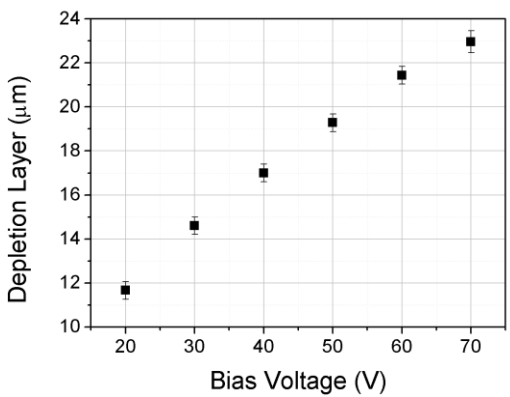


Contribution from the depletion layer

$$Q = Q_{\text{Depl}} + Q_{\text{Neutr}} \propto \left[\int_0^w \left(\frac{dE}{dx} \right) \cdot dx \right] + \left[\int_w^d \left(\frac{dE}{dx} \right) \cdot \exp \left[-\frac{x - W}{L_p} \right] \cdot dx \right]$$

Active region width

minority carrier diffusion length



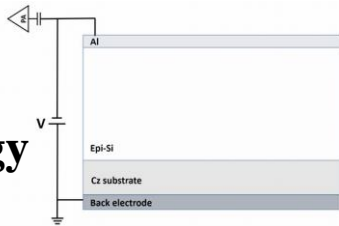
$L_p = (9.0 \pm 0.3) \mu\text{m}$
 $D_p = 3 \text{ cm}^2/\text{s}$
 $\tau_p = 270 \text{ ns}$

4H-SiC Schottky diode

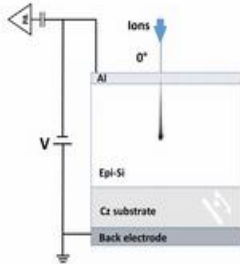


Parameter space: (E, θ , V)

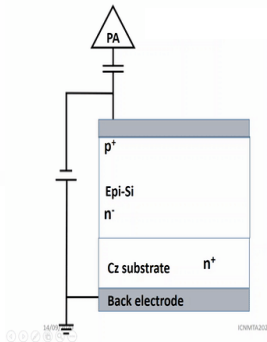
E
ion energy



θ
Tilting angle

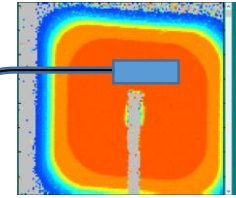


V
Bias voltage



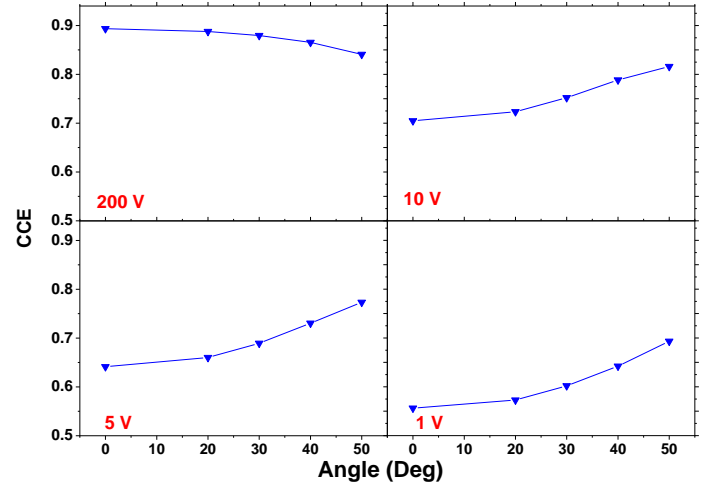
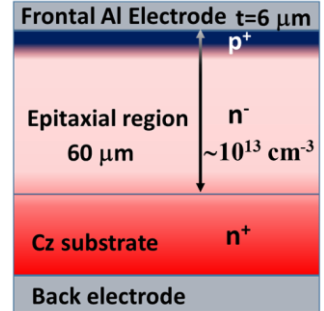
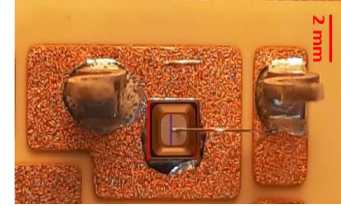
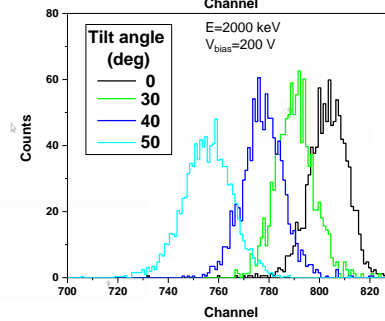
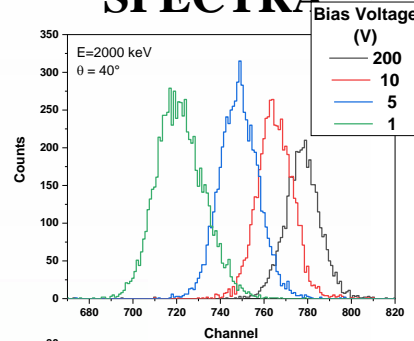
For each (E)

Selecting a region



IBIC Map

IBIC SPECTRA

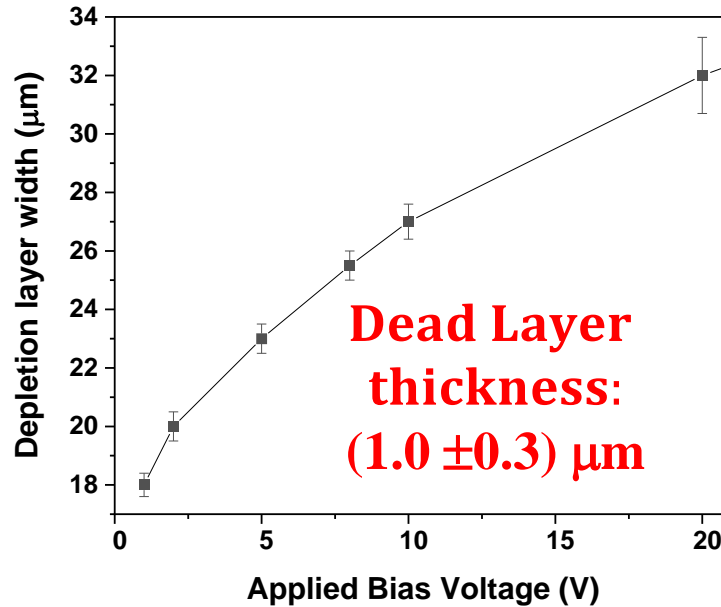




UNIVERSITÀ DI TORINO

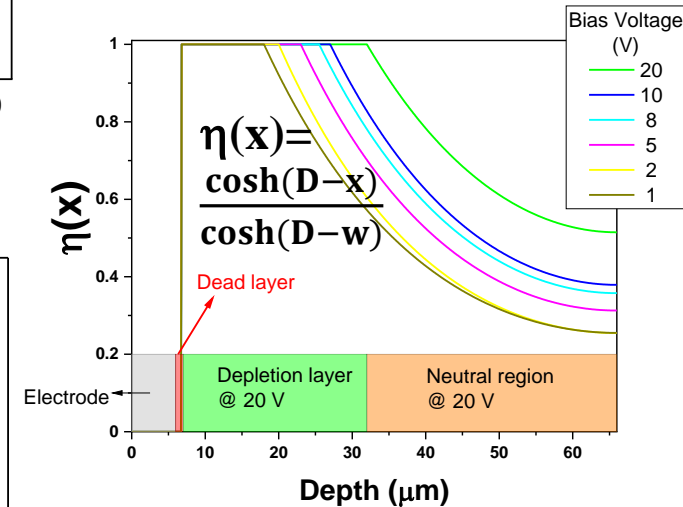


Behavior of the depletion layer width as function of the applied bias voltage



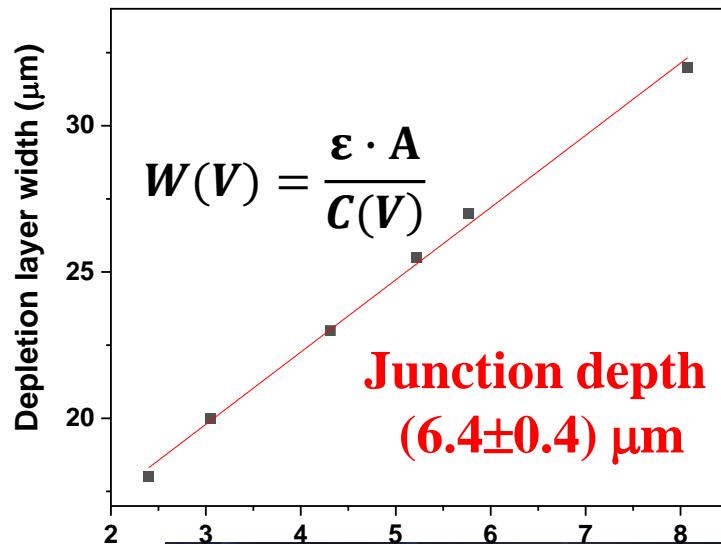
Model based on the Diffusion-drift model

Charge collection efficiency profiles at different bias voltages



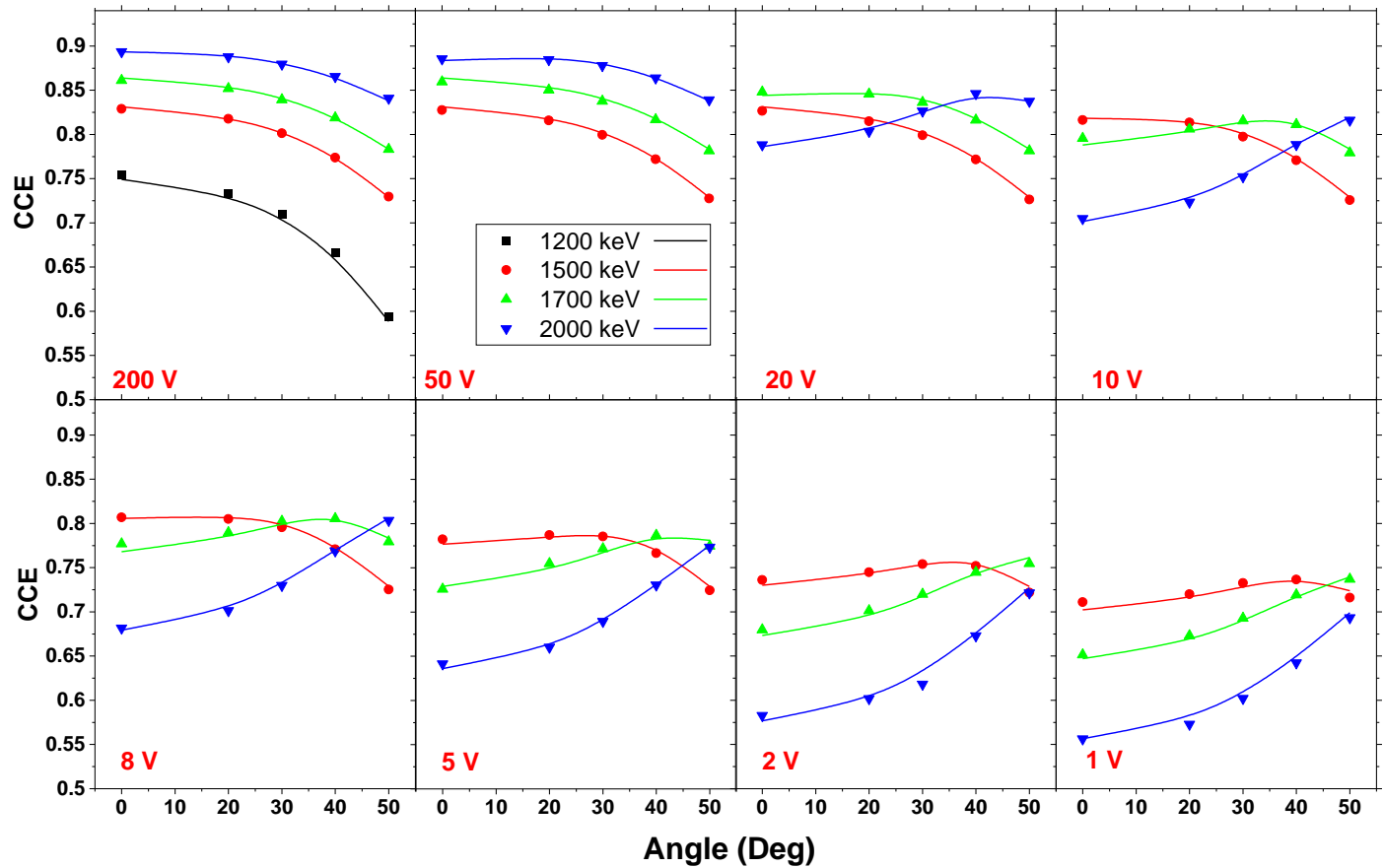
Minority carriers (holes) diffusion length: $L_h = (24.0 \pm 1.3) \mu\text{m}$

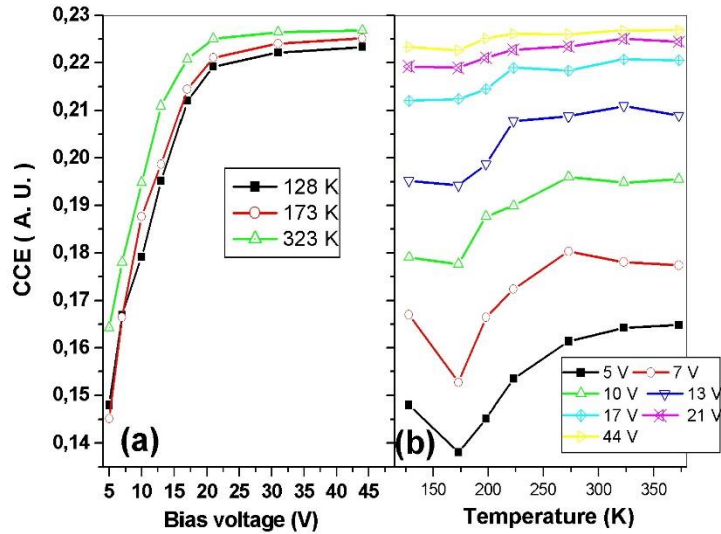
Linear relationship between inverse of capacitance and the depletion layer width



Experimental and fitting CCE as function of Tilting angle θ @ different V Parametrized by E

Solid lines are fitting curves



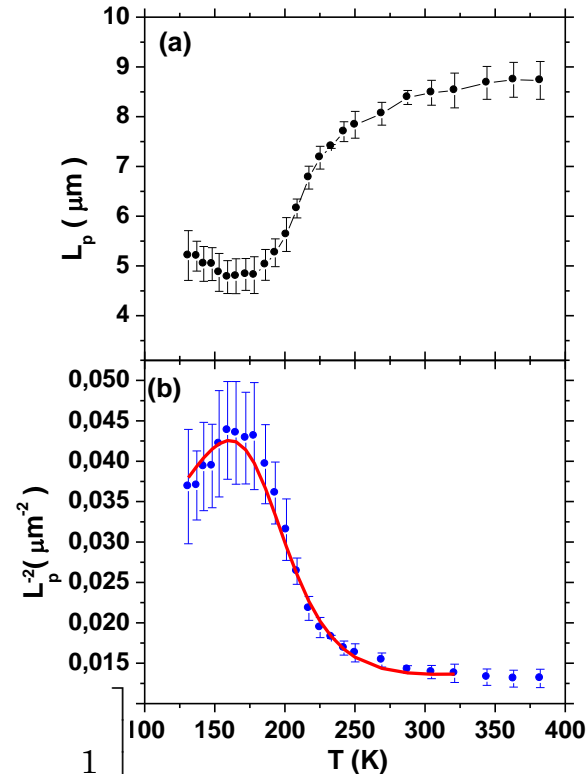


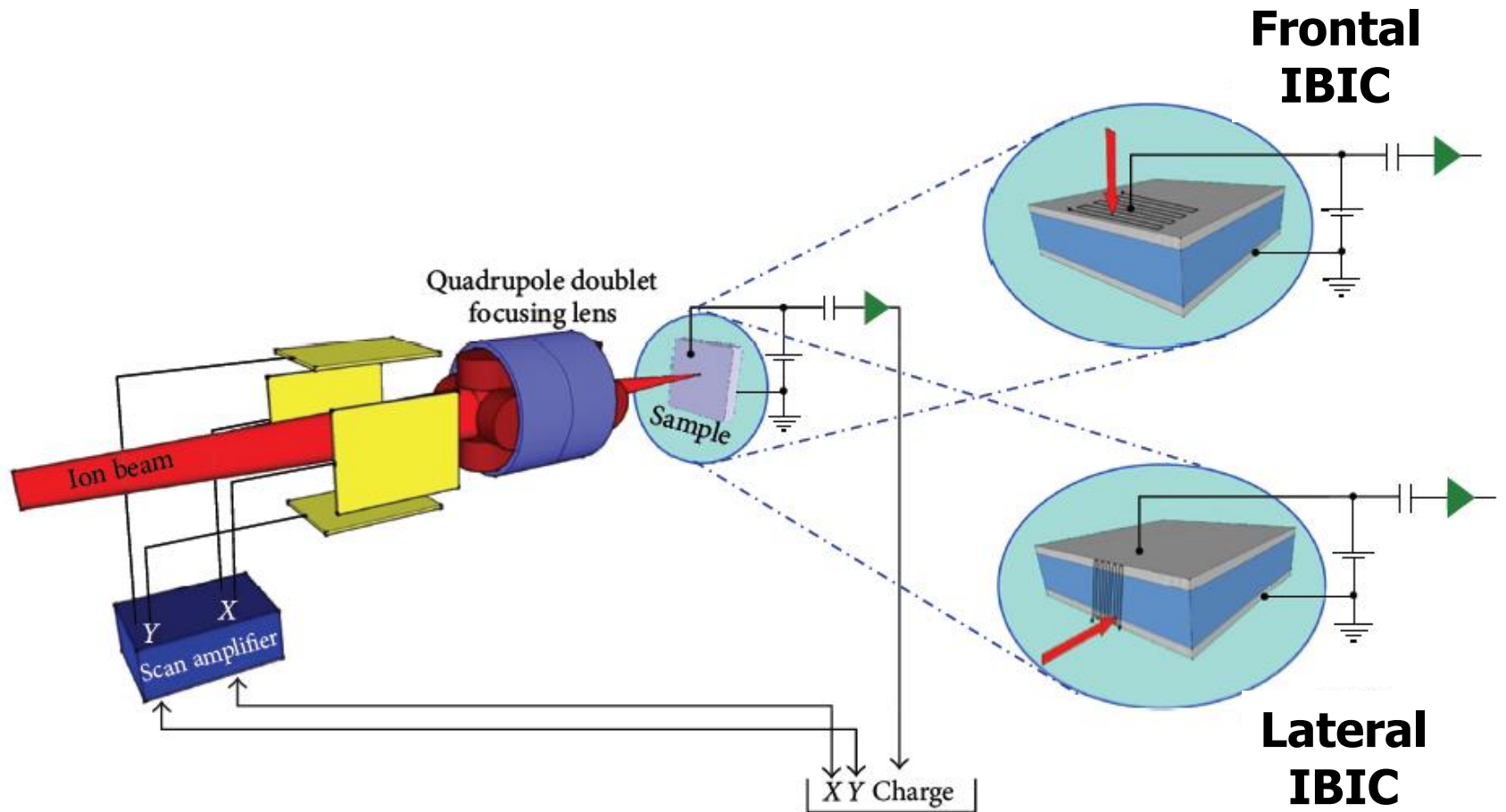
Two trapping levels

SRH recombination model

$$\frac{1}{L_p^2} = \frac{1}{D_p \cdot \tau} = \frac{1}{D_p} \cdot \left(\frac{1}{\tau(T)} + \frac{1}{\tau_B} \right) = A \cdot \frac{1}{T^{-0.5}} \cdot \left[\frac{1}{T^{-0.5} + \frac{B}{N_D} \cdot T \cdot \exp\left(-\frac{E_t}{k_B T}\right)} + \frac{1}{\tau_B} \right]$$

The fitting procedure provides a trapping level of about 0.163 eV which is close to the value found in similar 4H SiC Schottky diodes by DLTS technique (S1 level).







UNIVERSITÀ
DI TORINO



NIMB 537 (2023) 14

4H-SiC Schottky diode radiation hardness assessment by IBIC microscopy

Ettore Vittone^{a,*}, Paolo Olivero^a, Milko Jakšić^b, Željko Pastuović^c

Laboratory for Ion Beam Interactions, Ruder Boškovic Institute, Zagreb, Croatia

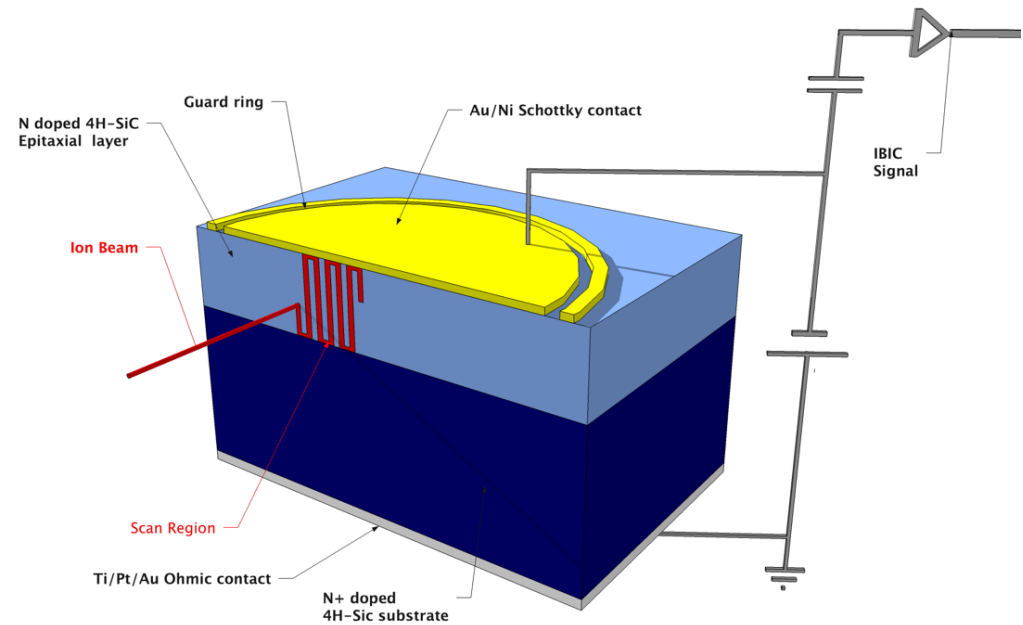
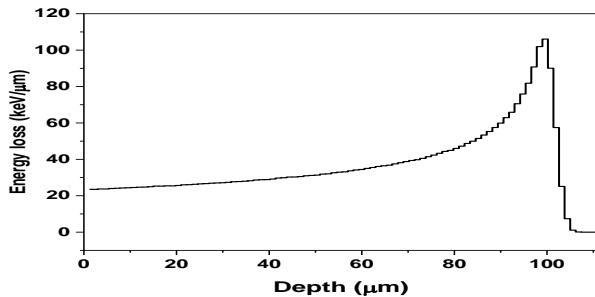
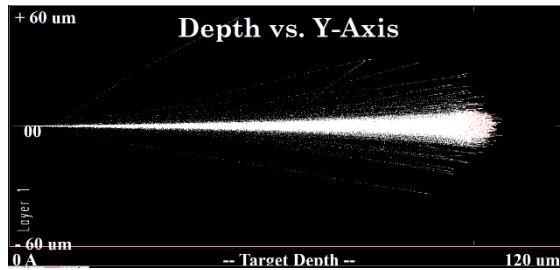


4 MeV protons

2 μm beam spot size (FWHM)

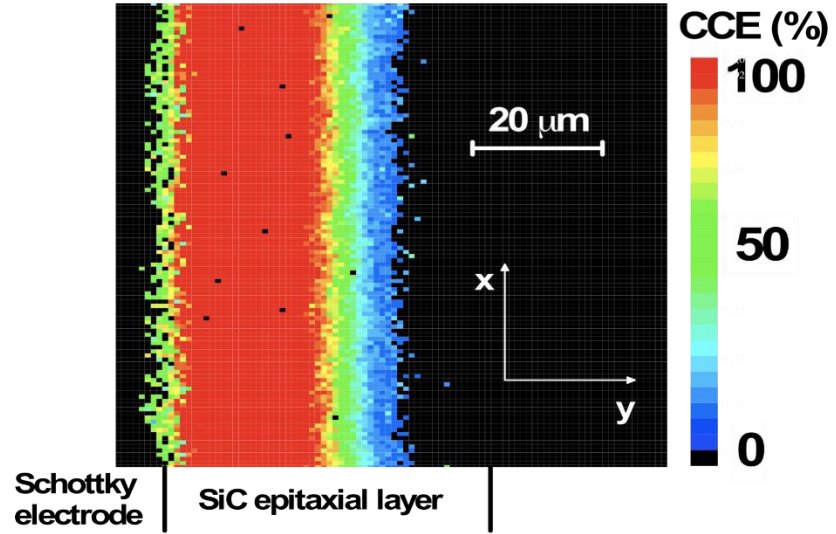
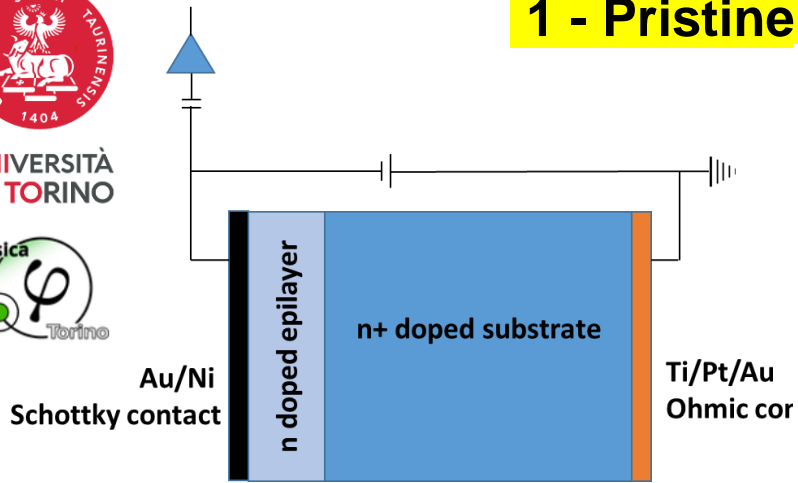
Charge sensitivity 1800 electrons/channel -> 14 keV in SiC

Spectral resolution: 12000 electrons (FWHM) ->94 keV in SiC

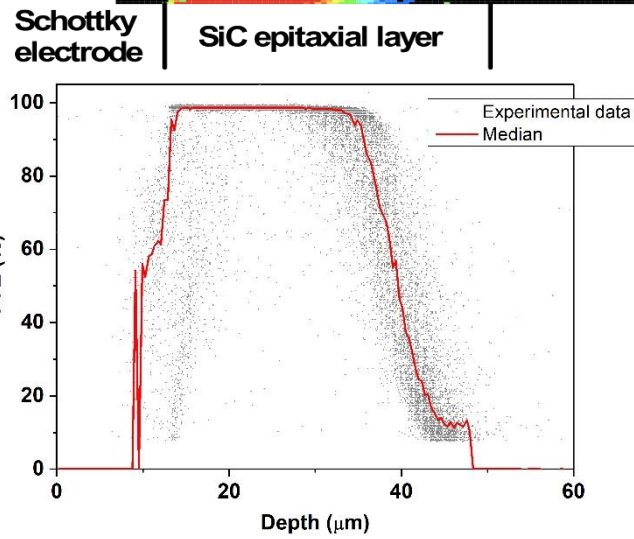
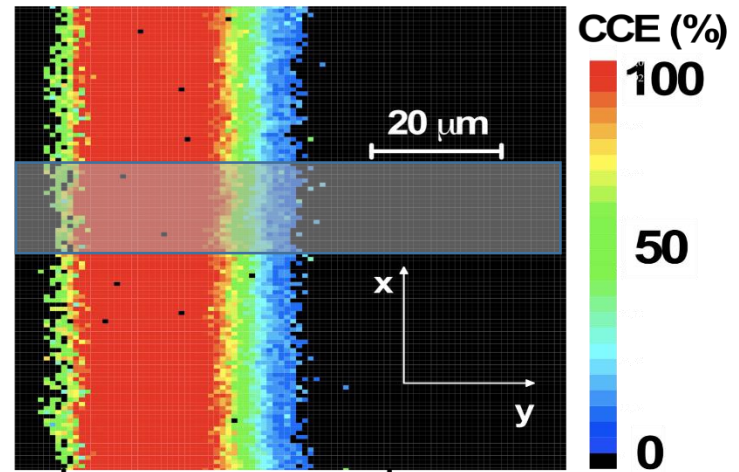
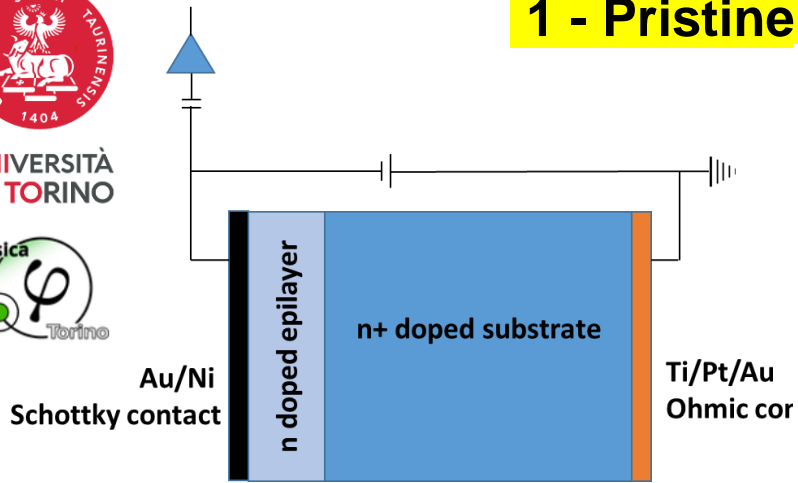


Range
Longitudinal: 100 μm
Lateral: 2.6 μm

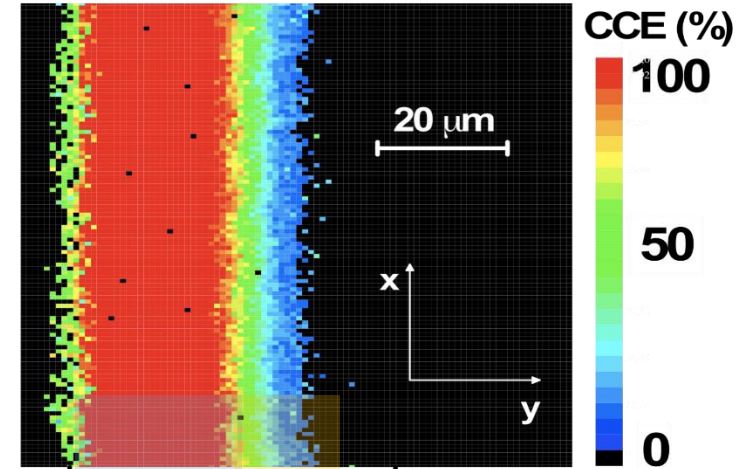
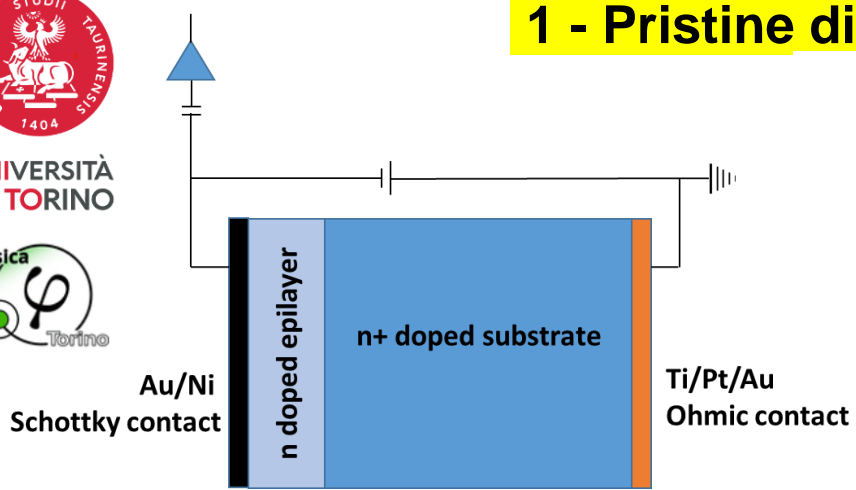
1 - Pristine diode: Lateral IBIC



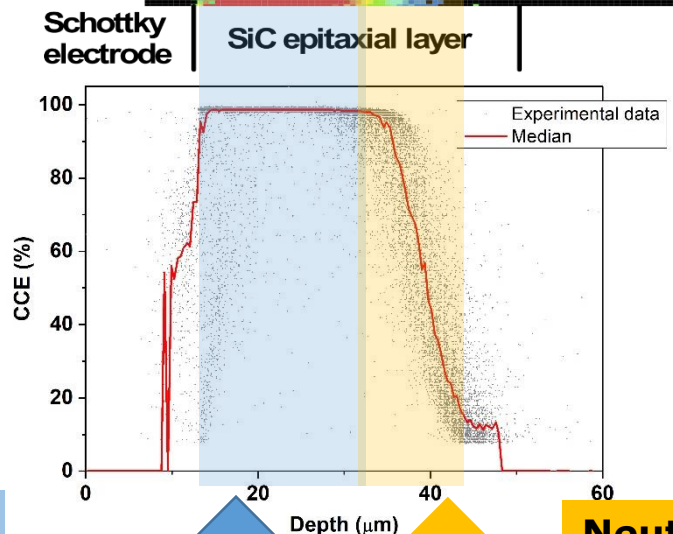
1 - Pristine diode: Lateral IBIC



1 - Pristine diode: Lateral IBIC



Drift-Diffusion model



Depletion layer

↓

high electric field/drift velocity

↓

Complete induced charge collection (Ramo theorem)

Neutral layer

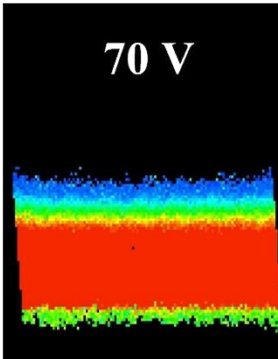
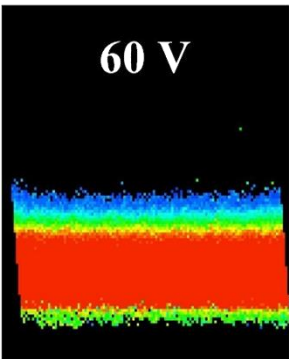
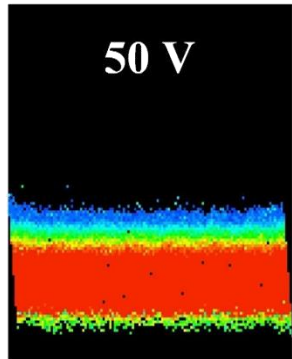
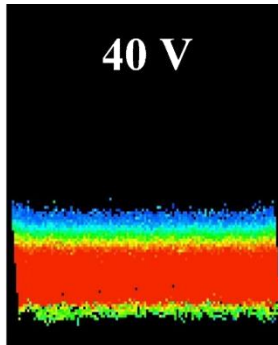
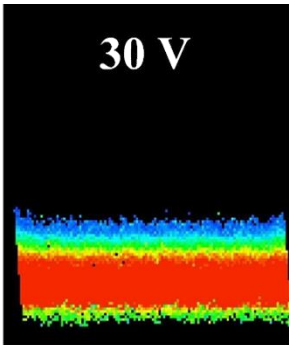
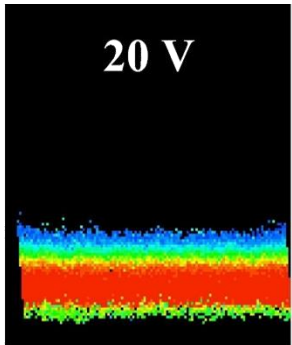
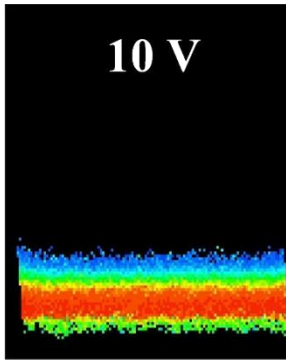
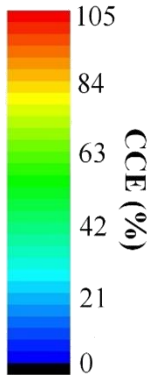
↓

Minority carrier diffusion

↓

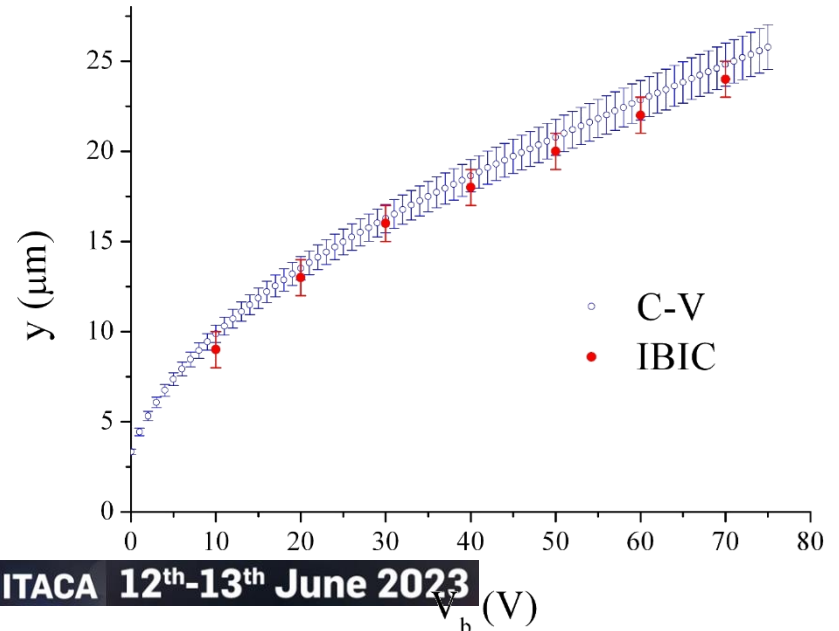
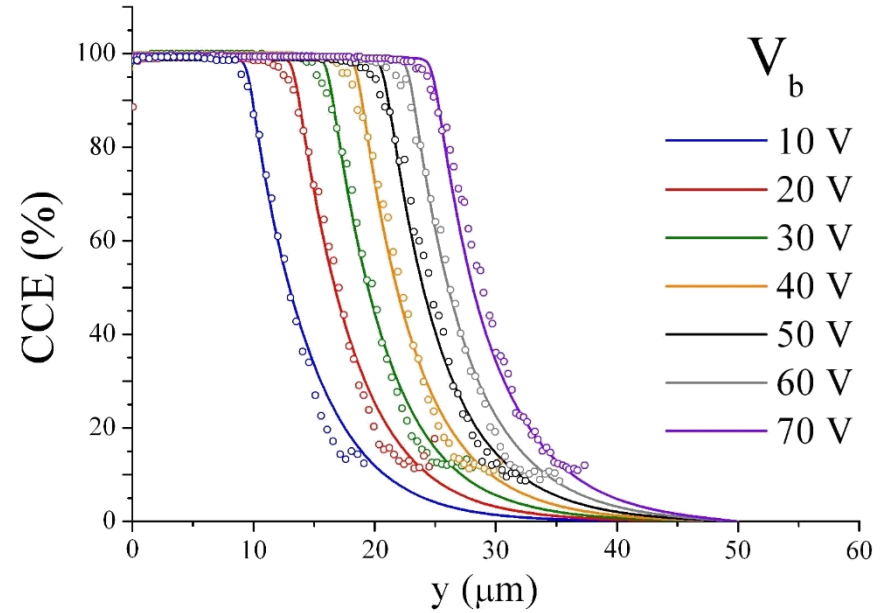
CCE exponential decay

20 μm
20 μm



Drift-diffusion model Simulation

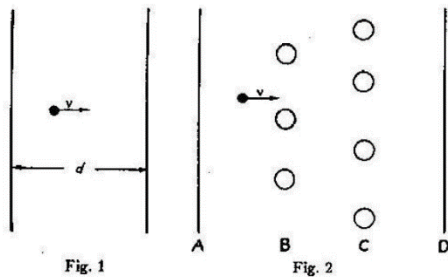
$$L_p = (4,9 \pm 0,3) \mu\text{m} \quad \tau_p \approx 80 \text{ ns}$$



Currents Induced by Electron Motion*

SIMON RAMO†, ASSOCIATE MEMBER, I.R.E.

Proc. of the IRE (1939), 584



Currents to Conductors Induced by a Moving Point Charge

W. SHOCKLEY

Bell Telephone Laboratories, Inc., New York, N. Y.

Journ. Appl. Phys. 9,(1938), 635

$$i = evE_0 = \frac{ev}{d}$$

Solid-State Electronics Pergamon Press 1964. Vol. 7, pp. 739-742. Printed in Great Britain

A GENERAL EXPRESSION FOR ELECTROSTATIC INDUCTION AND ITS APPLICATION TO SEMICONDUCTOR DEVICES

J. B. GUNN

$$\nabla_r Q_i = -q \left\{ \frac{\partial E}{\partial V_i} \right\} v \quad (7)$$

Nuclear Instruments and Methods in Physics Research A 428 (1999) 72-80

Theoretical framework for mapping pulse shapes in semiconductor radiation detectors

T.H. Prettyman*

$$\frac{\partial n^+}{\partial t} = \mu_n \nabla \varphi \cdot \nabla n^+ + \nabla \cdot (D_n \nabla n^+) - n^+ / \tau_n + G_n^+ \quad (6)$$

where n^+ is the adjoint electron concentration. If

$$n^+(r, t) = \eta_{nk}(r, t) \quad (7)$$

In other words, all of the charge pulses that can be produced by a detector for impulses of charge at discrete locations can be determined by solving a single, time-dependent problem.

Nuclear Instruments and Methods in Physics Research B 161–163 (2000) 446–451

Theory of ion beam induced charge collection in detectors based on the extended Shockley–Ramo theorem

E. Vittone ^{a,b,*}, F. Fizzotti ^a, A. Lo Giudice ^{a,b}, C. Paolini ^a, C. Manfredotti ^{a,b}

Materials Science and Engineering B102 (2003) 193–197

Time-resolved ion beam-induced charge collection measurement of minority carrier lifetime in semiconductor power devices by using Gunn's theorem

C. Manfredotti ^{a,*}, F. Fizzotti ^a, A. Lo Giudice ^a, M. Jaksic ^b, Z. Pastuovic ^b, C. Paolini ^a, P. Olivero ^a, E. Vittone ^a

Nuclear Instruments and Methods in Physics Research B 219–220 (2004) 1043–1050

Theory of ion beam induced charge measurement in semiconductor devices based on the Gunn's theorem

E. Vittone ^{*}

Nuclear Instruments and Methods in Physics Research B 264 (2007) 345–360

A review of ion beam induced charge microscopy

M.B.H. Breese ^{a,*}, E. Vittone ^b, G. Vizkelethy ^c, P.J. Sellin ^d

Nuclear Instruments and Methods in Physics Research B 332 (2014) 257–260

A Monte Carlo software for the 1-dimensional simulation of IBIC experiments

J. Forneris ^{a,*}, M. Jakšić ^b, Ž. Pastuović ^c, E. Vittone ^a



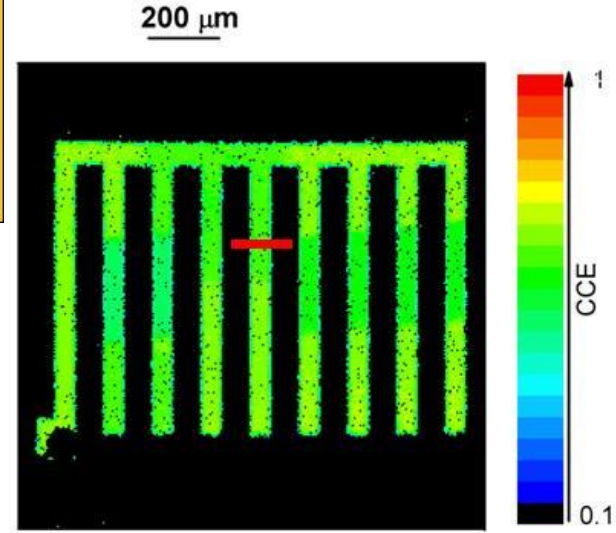
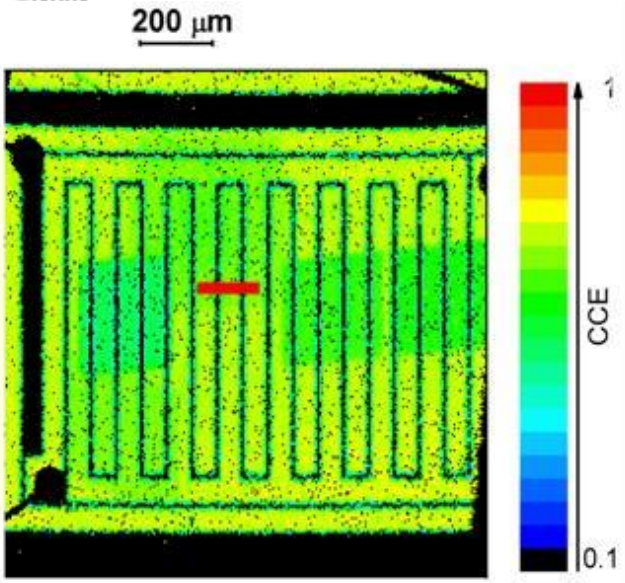
Experiments to validate the theoretical model



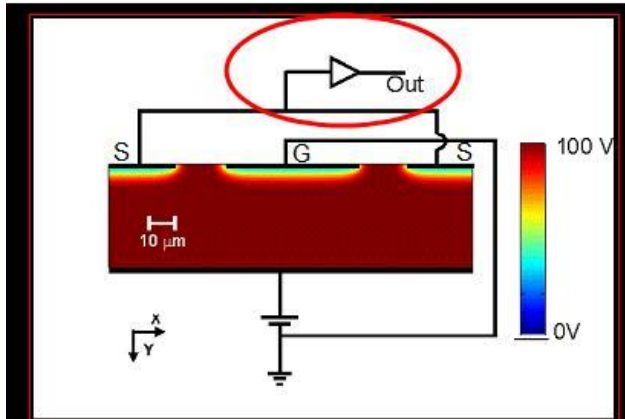
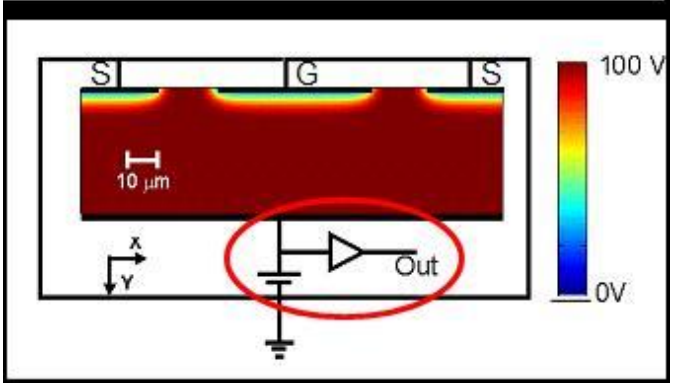
SEM image 4H-SiC Schottky diode

Inter-digitated frontal electrodes

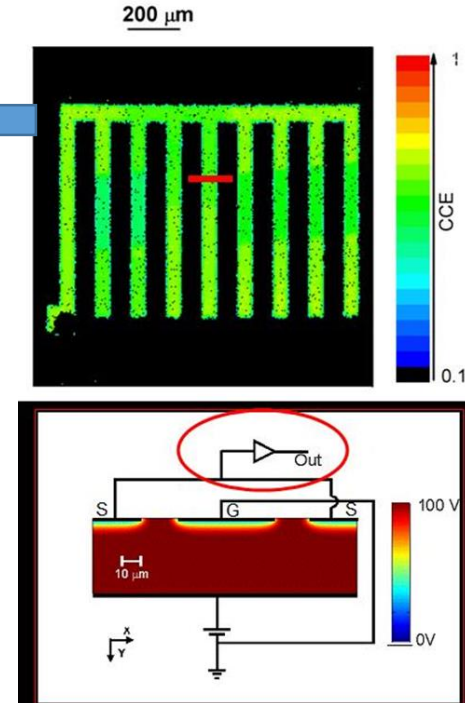
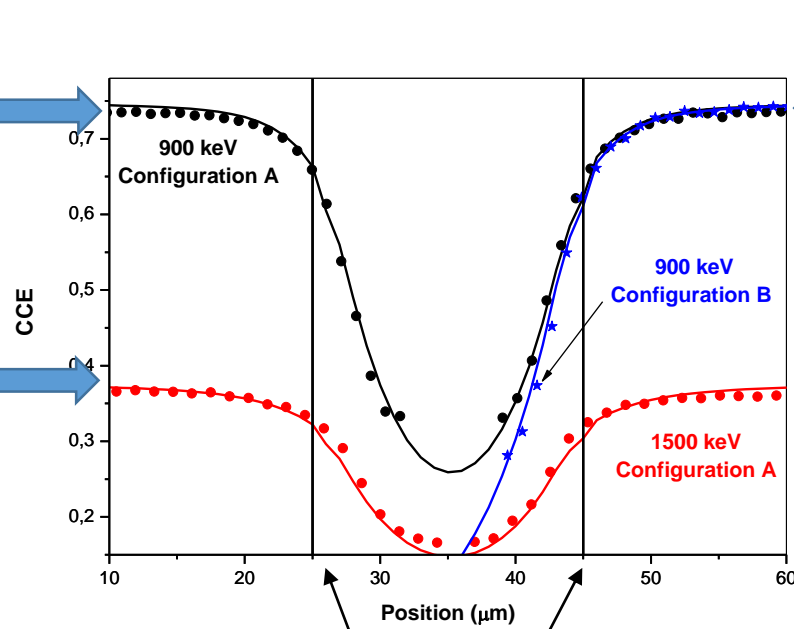
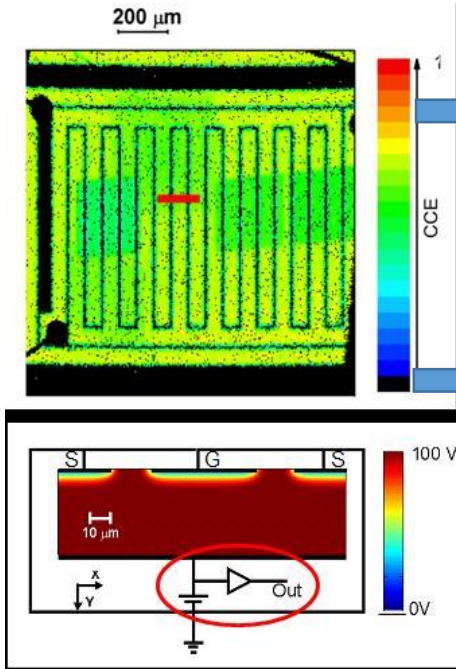
- Finger width: 50 μm
- Finger length: 700 μm
- Finger-finger gap = 20 μm ;
- Finger-guard ring = 70 μm .



IBIC map
1.5 MeV H⁺



Electrostatic
Potential map
 $V_{\text{bias}}=100\text{V}$



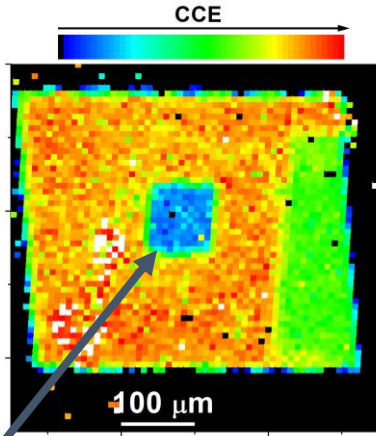
Electrode edges.



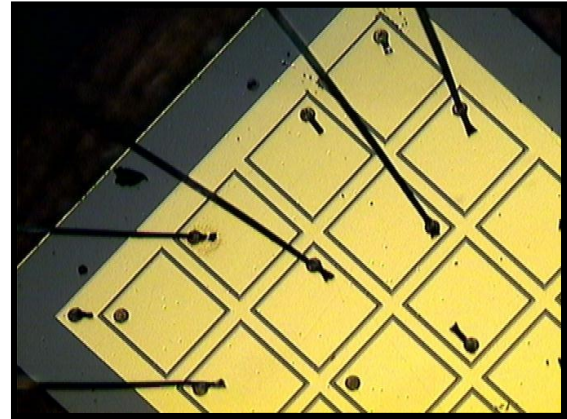
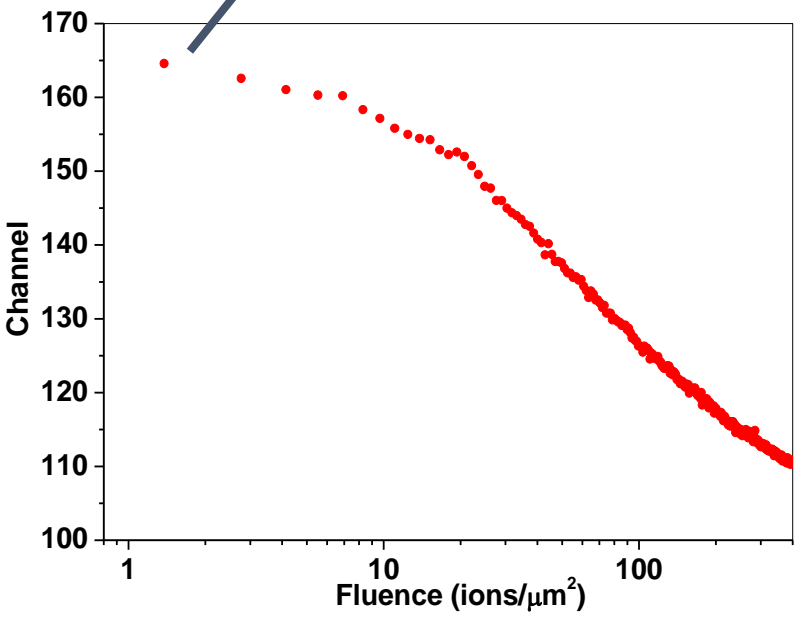
UNIVERSITÀ
DI TORINO

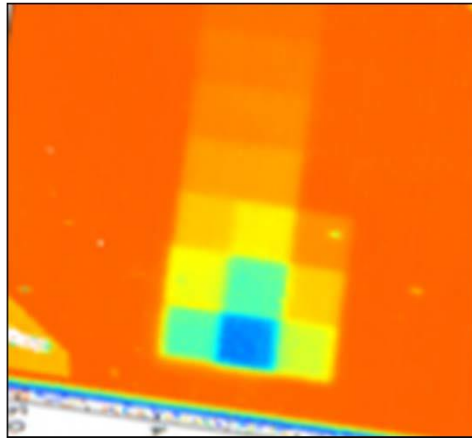


Functionalization of semiconductor materials



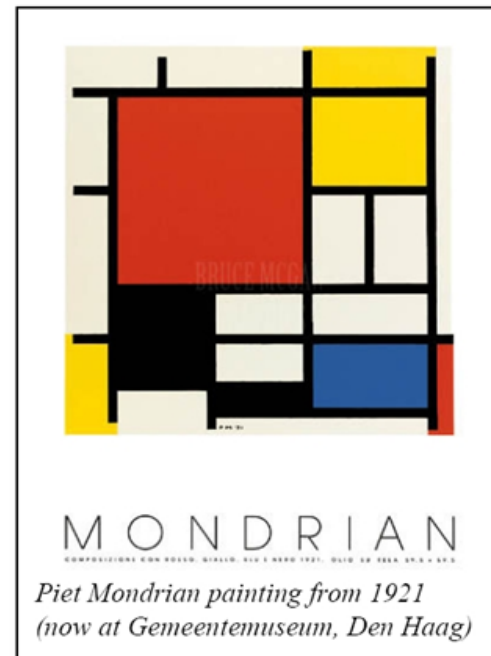
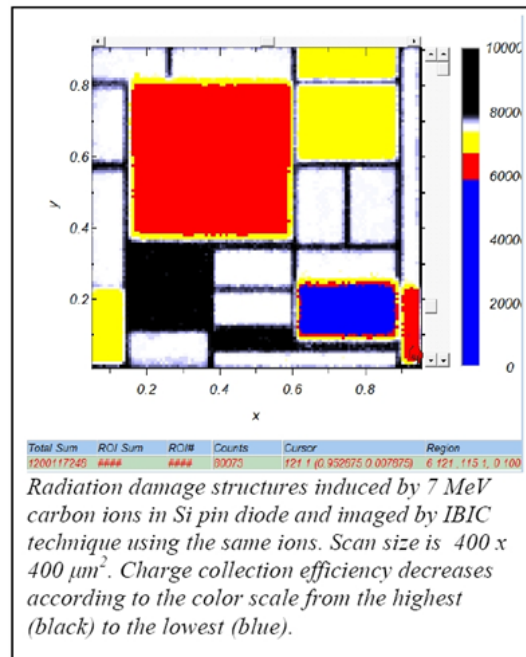
2 MeV H⁺ IBIC Map of 400x400 μm² 4H-SiC Schottky diode





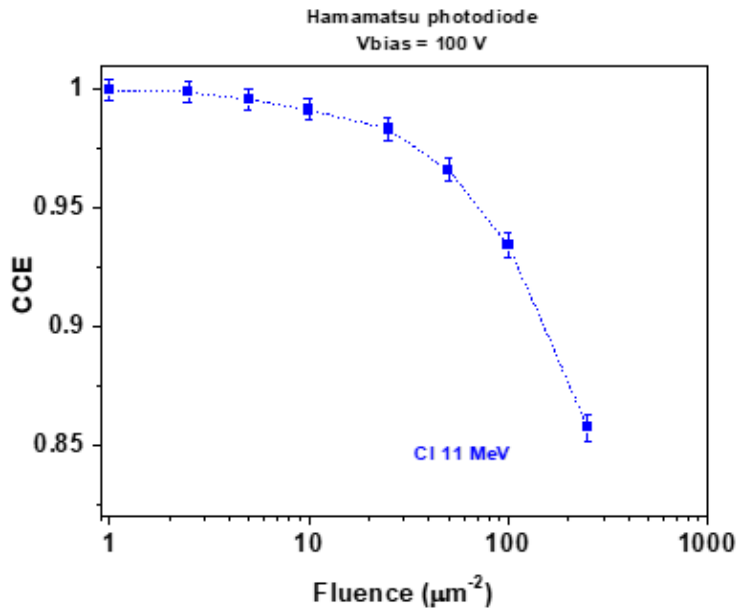
CCE map of a silicon photodiode with selected regions damaged with a) protons

IAEA – CRP, RBI Report

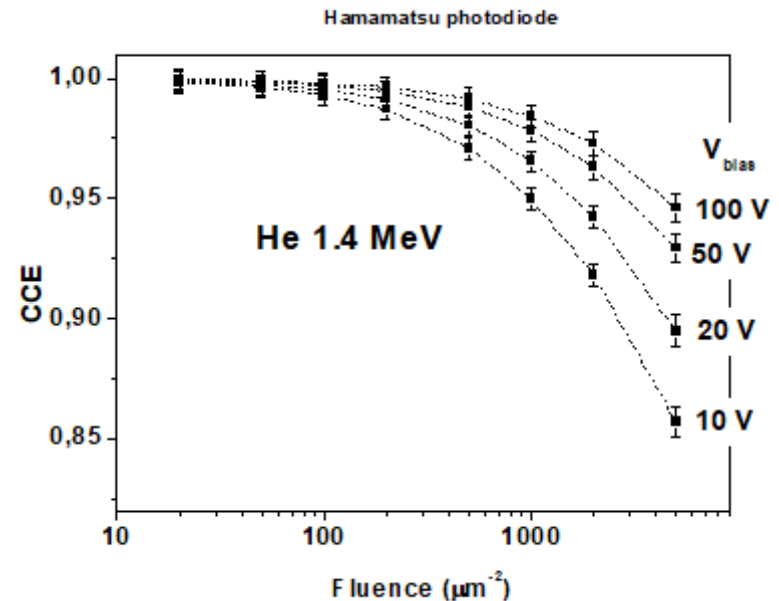


CCE degradation induced by ion irradiation

Depends on the damaging ion fluence

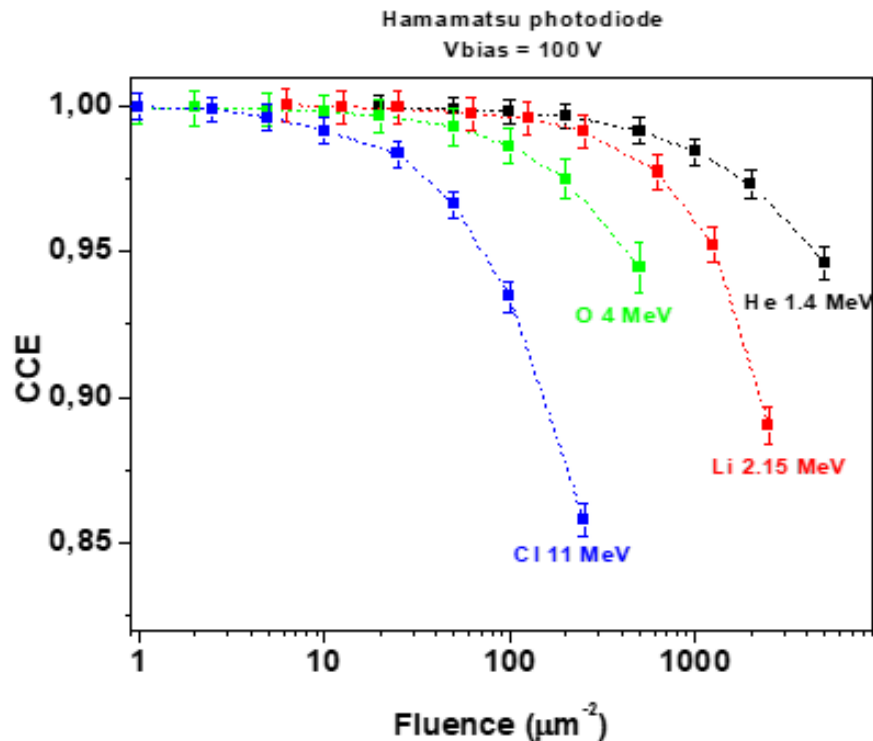


Depends on the polarization state

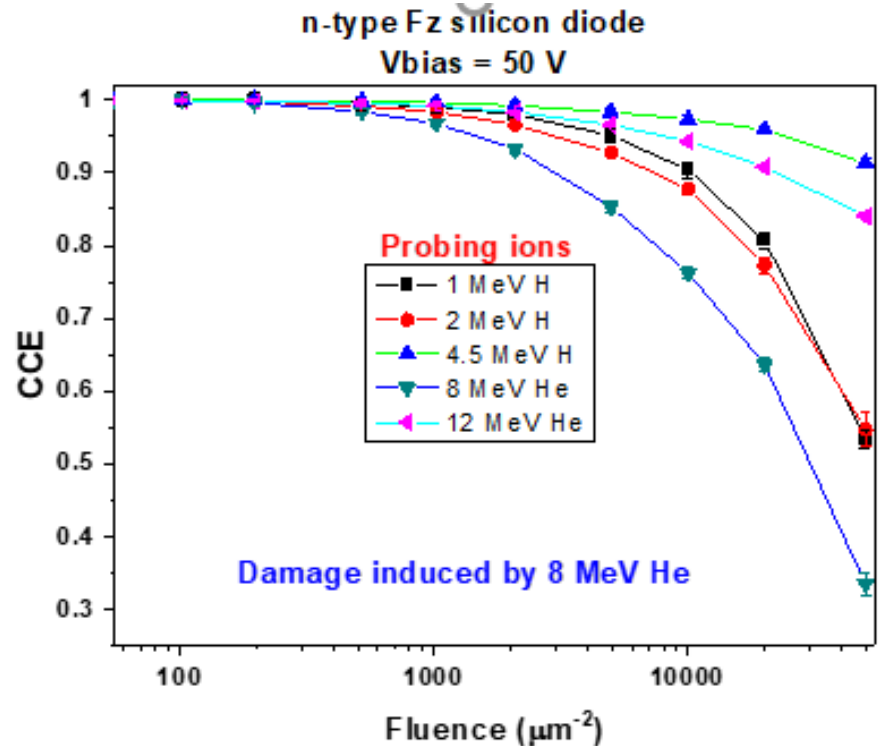


CCE degradation induced by ion irradiation

Depends on the damaging ion mass and energy



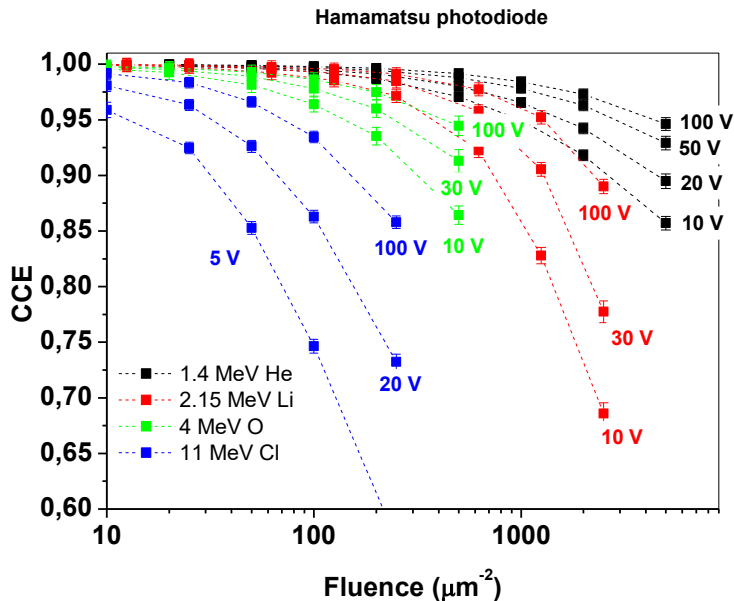
Depends on the probing ion mass and energy



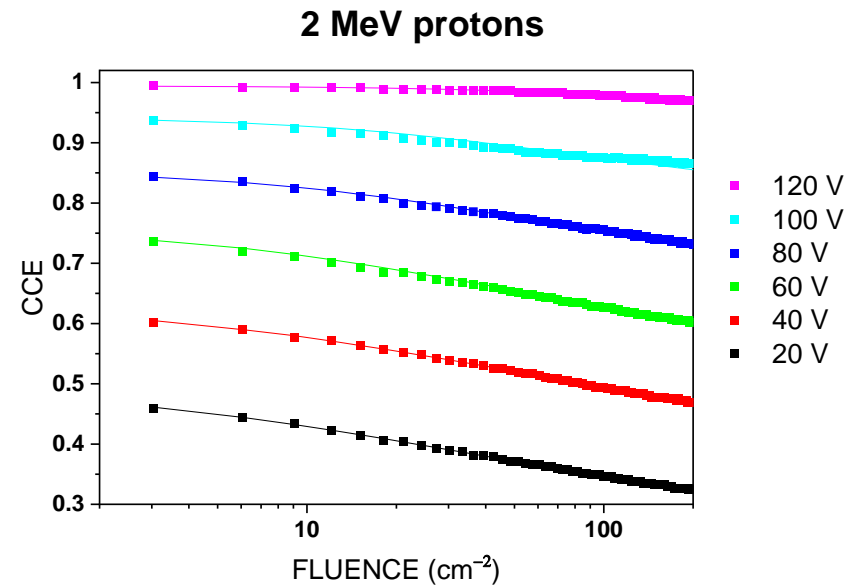
CCE degradation induced by ion irradiation

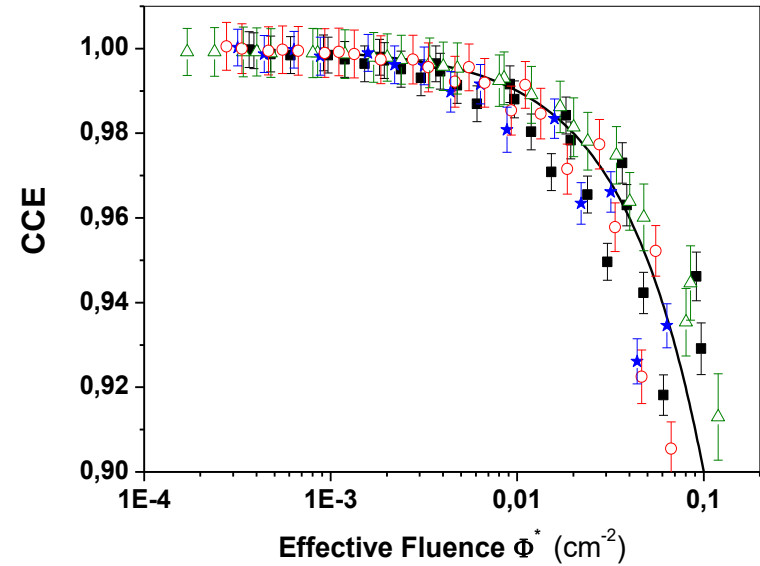
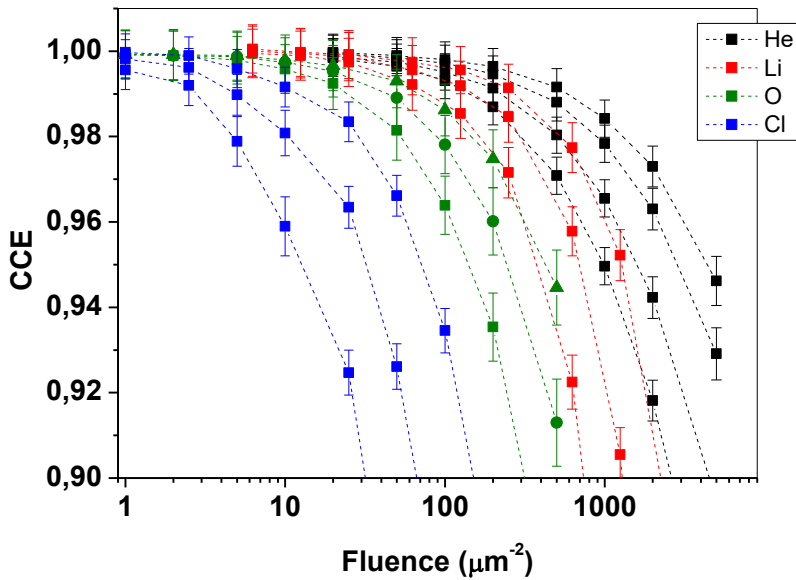
Depends on the material and/or device

Silicon pin photodiode



4H-SiC Schottky diode





$$CCE \cong 1 - K^* \cdot \Phi^*$$

From fit : effective damage factor $K^* = k_e \cdot \sigma_e = (8.4 \pm 0.3) \cdot 10^{16} \text{ cm}^2$.

From DLTS : $\sigma_e = 5 \cdot 10^{-15} \text{ cm}^2$

$k_e \cong 0.17$ active traps/vacancy

APL 98 092101 (2011)

Ettore Vittone

Probability of divacancy trap production in silicon diodes exposed to focused ion beam irradiation

Željko Pastuović,^{1,a)} Ettore Vittone,² Ivana Čapan,¹ and Milko Jakšić¹



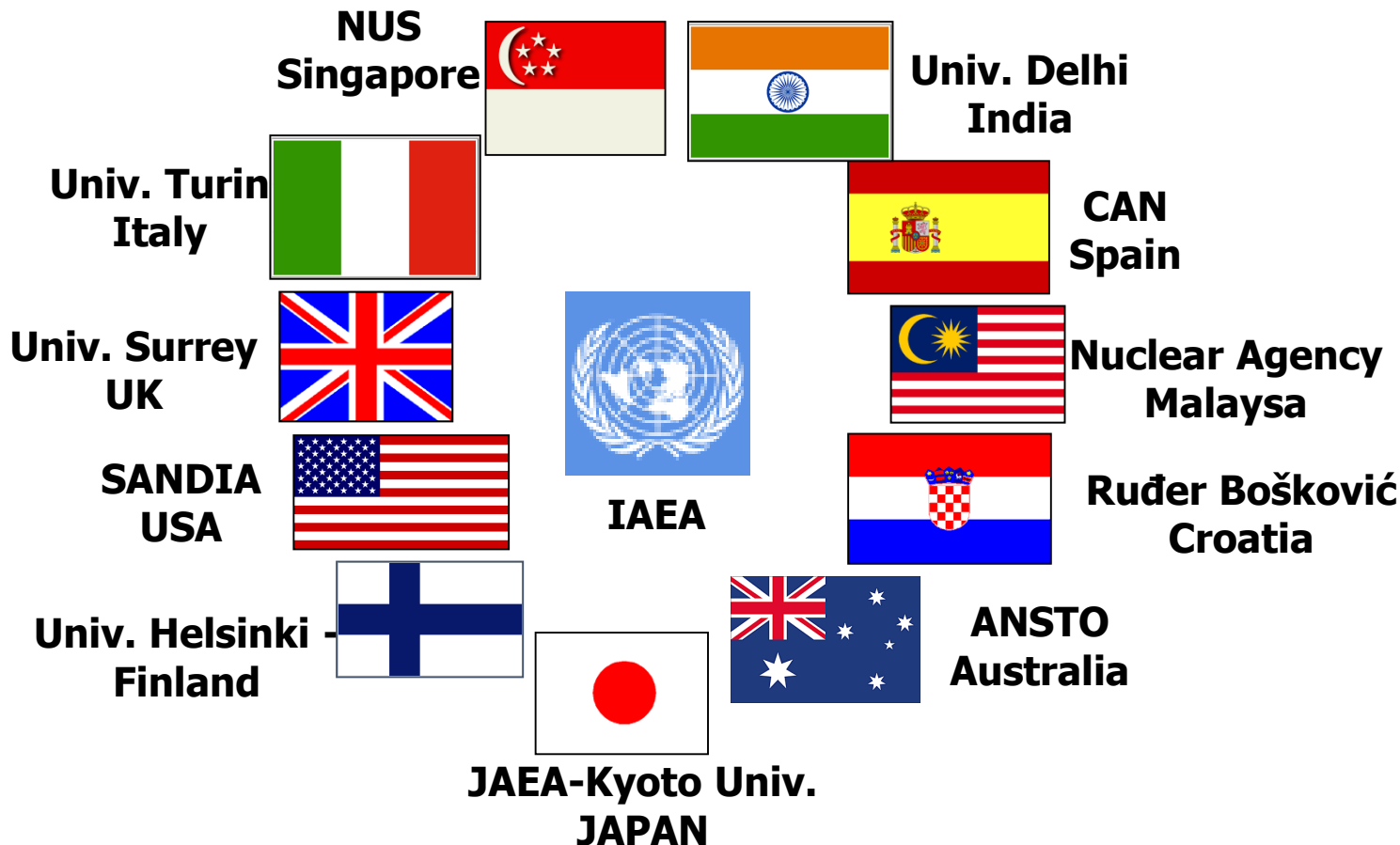
UNIVERSITÀ
DI TORINO



IAEA Coordinate Research Programme (CRP) F11016

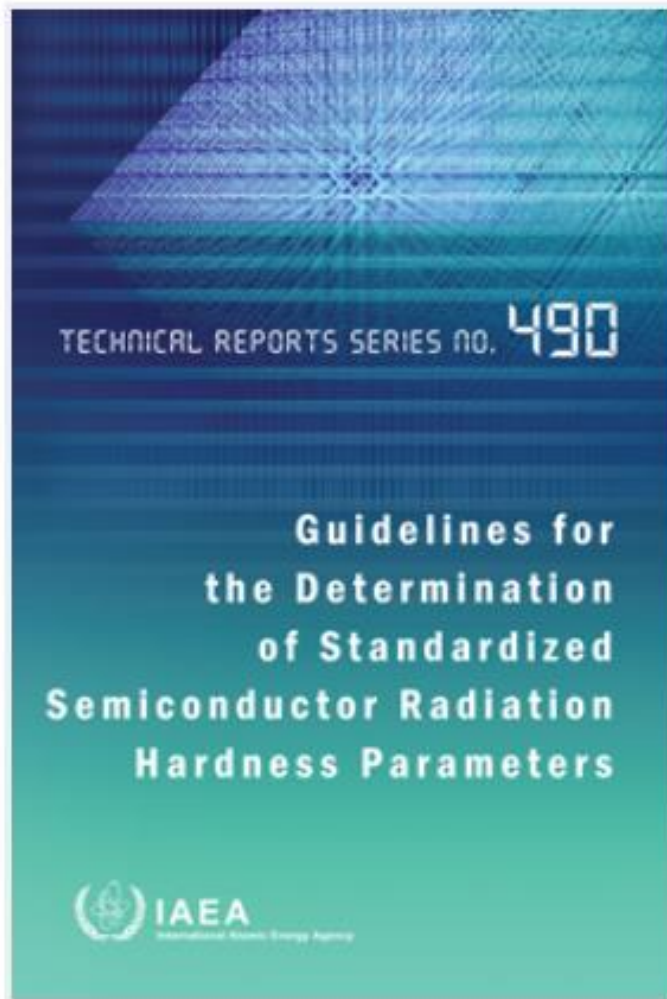
"Utilization of ion accelerators for studying and modeling of radiation induced defects in semiconductors and insulators"

**COOPERATION AND MUTUAL
UNDERSTANDING LEAD TO GROWTH AND
GLOBAL ENRICHMENT**





UNIVERSITÀ
DI TORINO



CONTRIBUTORS TO DRAFTING AND REVIEW

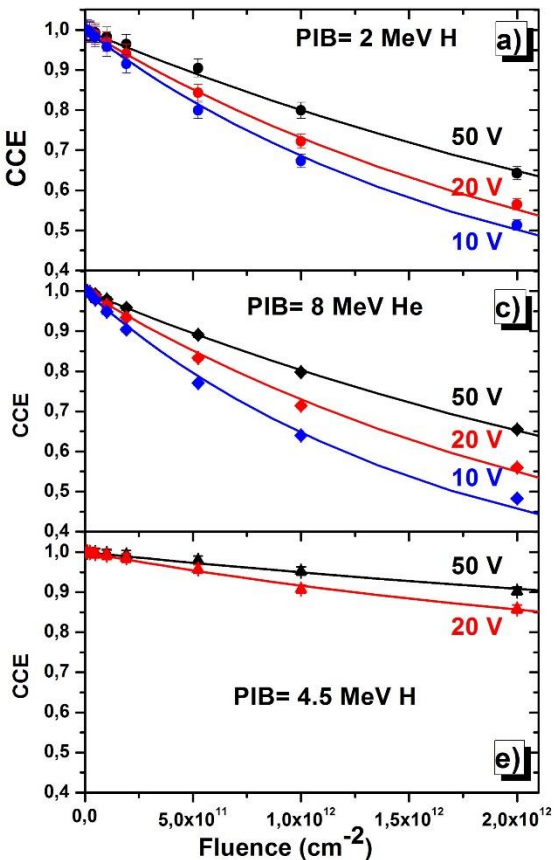
Garcia Lopez, J.	Centro Nacional de Aceleradores, University of Sevilla, Spain
Grilj, V.	Ruder Bošković Institute, Croatia
Jakšić, M.	Ruder Bošković Institute, Croatia
Jimenez Ramos, C.	Centro Nacional de Aceleradores, University of Sevilla, Spain
Lohstroh, A.	University of Surrey, United Kingdom
Pastuović, Ž.	Australian Nuclear Science and Technology Organisation, Australia
Rath, S.	University of Delhi, India
Siegele, R.	Australian Nuclear Science and Technology Organisation, Australia
Simon, A.	International Atomic Energy Agency
Skukan, S.	Ruder Bošković Institute, Croatia
Vittone, E.	University of Torino, Italy
Vizkelethy, G.	Sandia National Laboratories, United States of America

89 pages | 42 figures

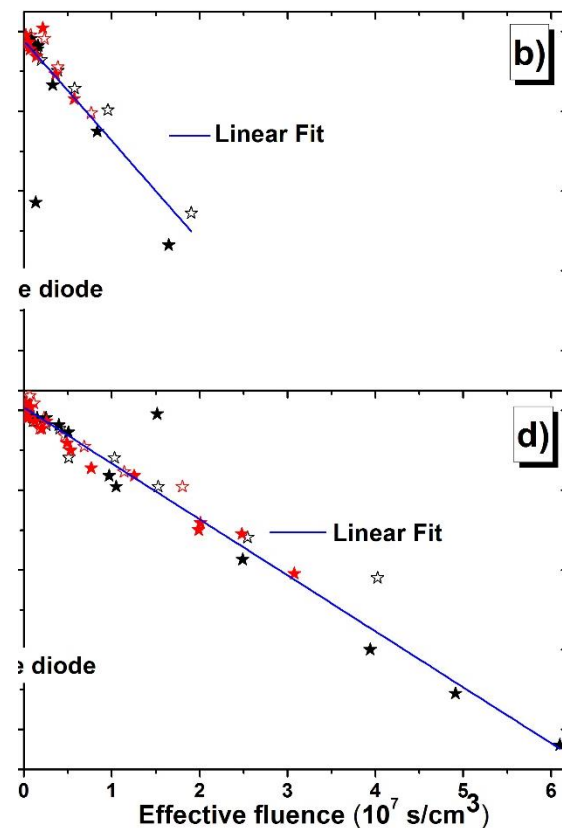
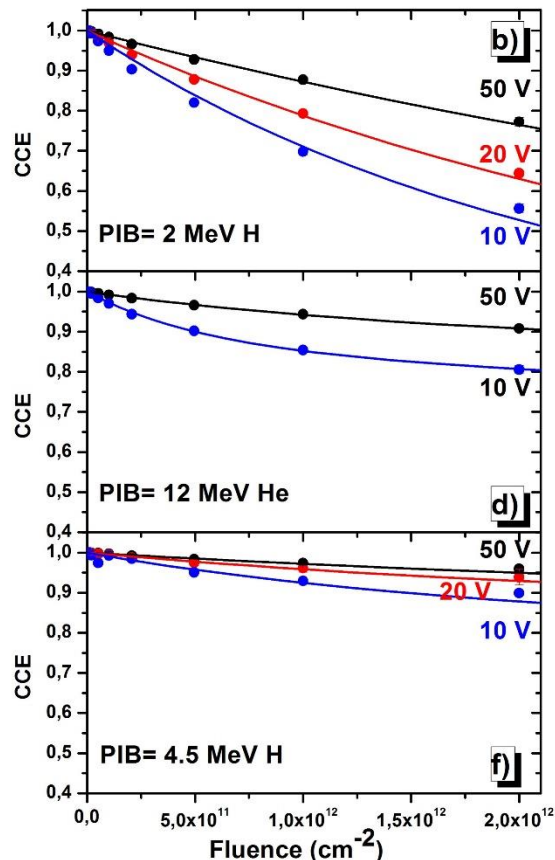
Date published: 2023

<https://www.iaea.org/publications/12356/guidelines-for-the-determination-of-standardized-semiconductor-radiation-hardness-parameters>

DIB: 8 MeV He



DIB: 4 MeV He

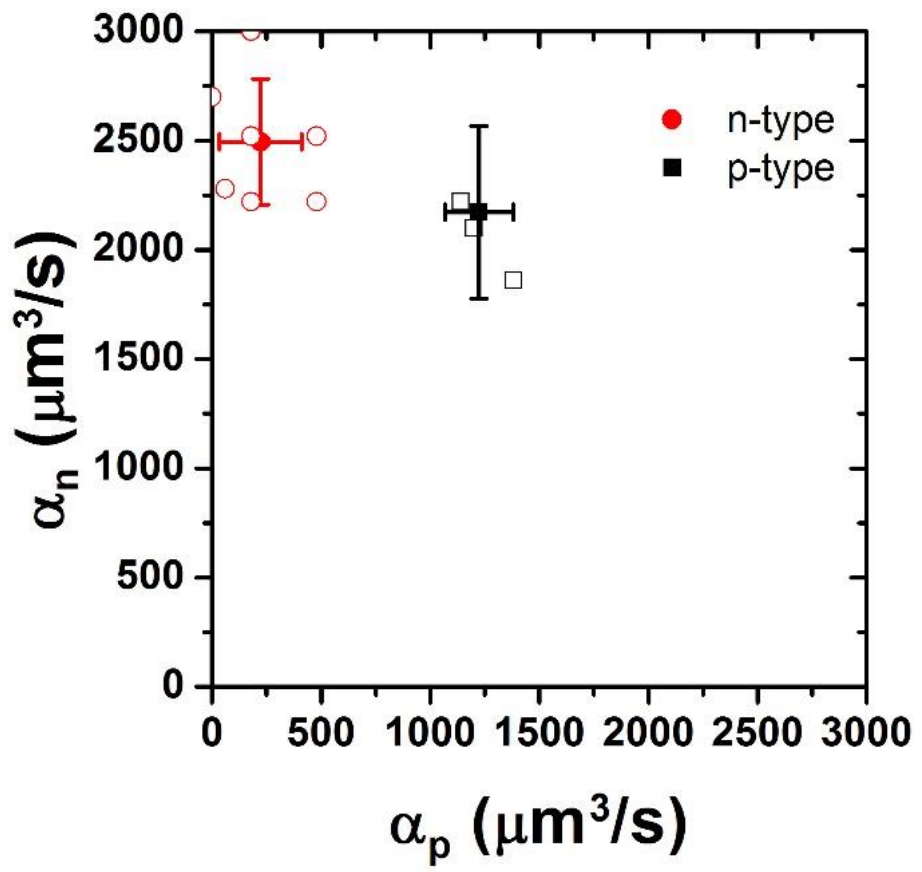


CCE degradation depends from

- **Damaging ion energy and mass**
- **Probing ion energy and mass**
- **Polarization**

The solid lines are the best fits obtained by means of our model considering

- Different PIBs
- Different DIBs (8 MeV, 4 MeV)
- Different polarizations (10,20,50 V)



Recombination coefficient
 $\alpha = k \cdot \sigma \cdot v_{th}$

Final measurement of the recombination coefficients;
 n-type diode: $\alpha_p = (210 \pm 160) \mu\text{m}^3/\text{s}$; $\alpha_n = (2500 \pm 300) \mu\text{m}^3/\text{s}$;
 p-type diode: $\alpha_n = (2200 \pm 300) \mu\text{m}^3/\text{s}$; $\alpha_p = (1310 \pm 90) \mu\text{m}^3/\text{s}$;
 Open marks: dispersion of the combination of the fitting parameters.



UNIVERSITÀ
DI TORINO

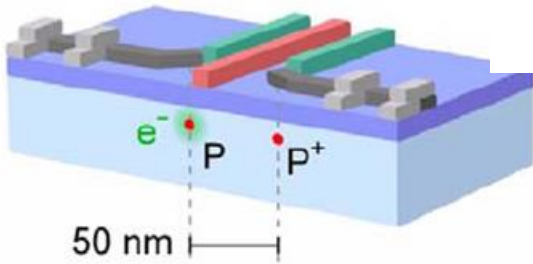


Ion beam characterization by functionalized devices (by ion beams)

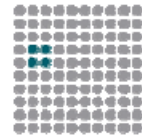


UNIVERSITÀ
DI TAVERNA

The two atom device

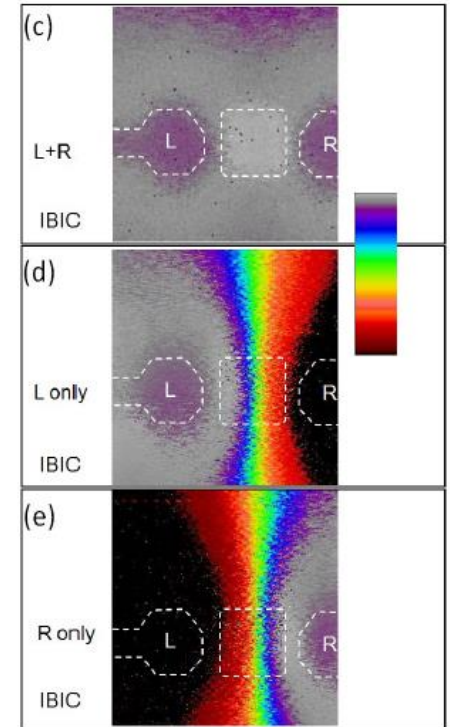
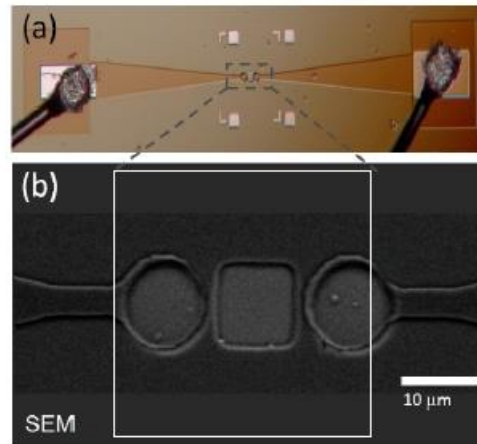
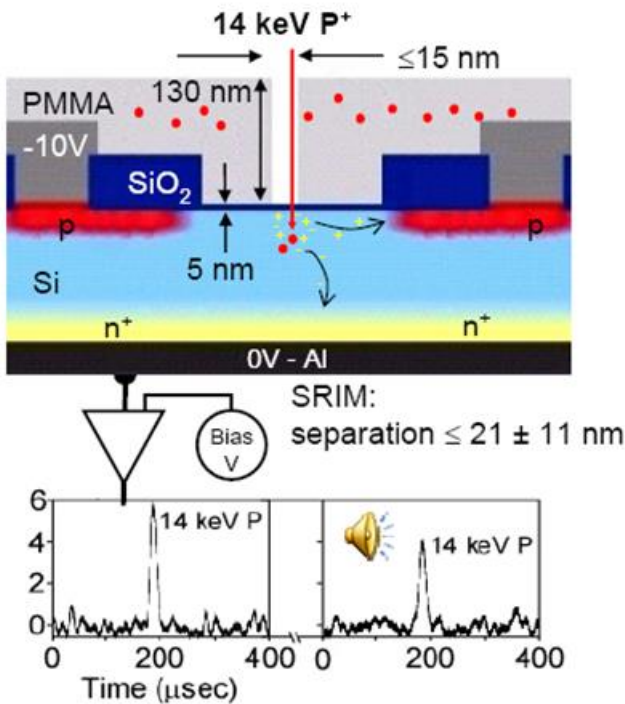
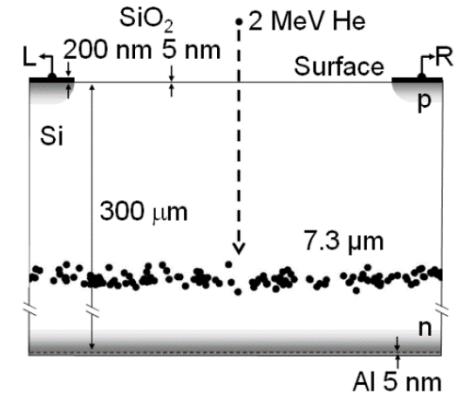


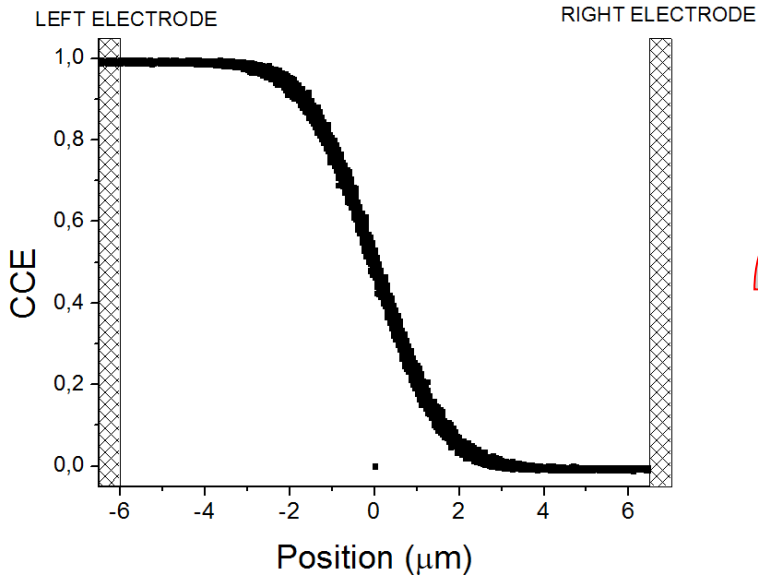
David N. Jamieson
School of Physics
University of Melbourne



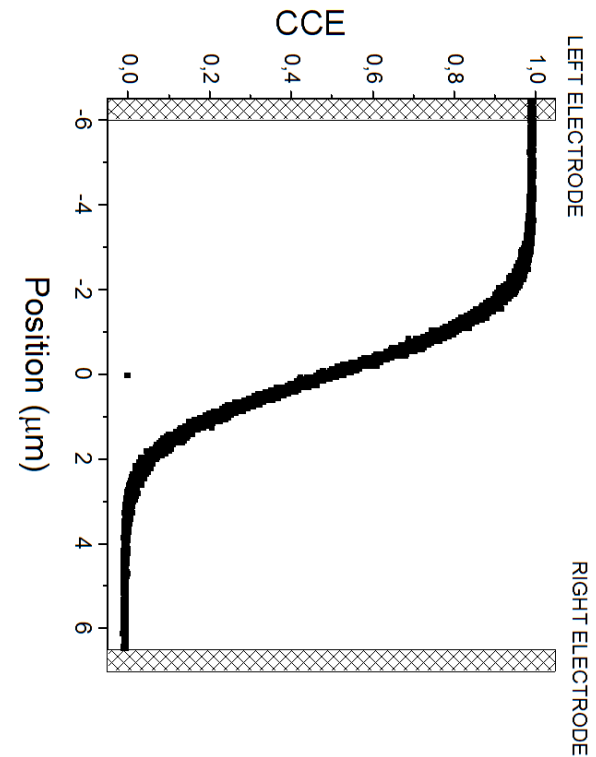
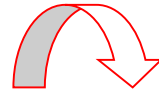
CENTRE FOR
QUANTUM COMPUTER
TECHNOLOGY
AUSTRALIAN RESEARCH COUNCIL CENTRE OF EXCELLENCE

Position sensitivity - proof of concept: three-electrodes test device
L.M. Jong et al., Nuclear Instr. Meth. B 269 (2011) 2336





CCE AS FUNCTION OF ION STRIKE POSITION

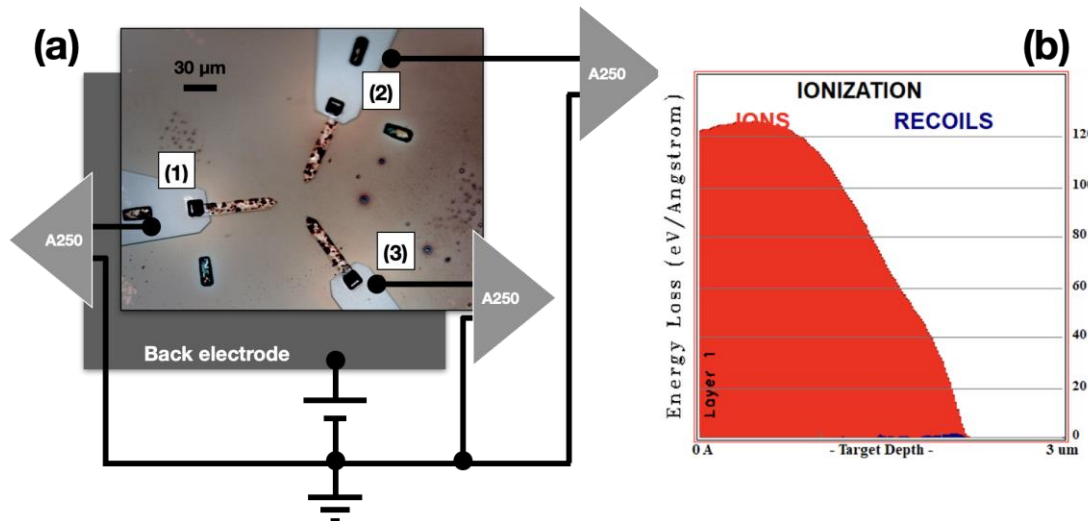
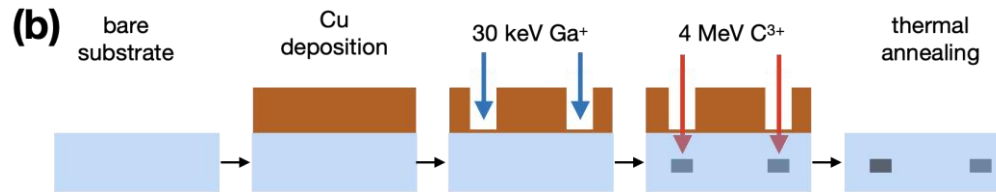
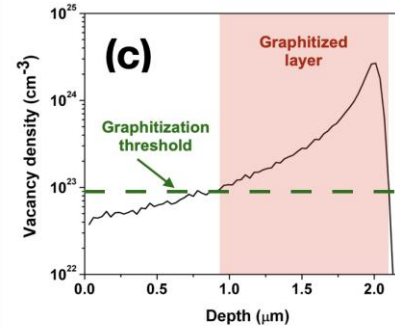
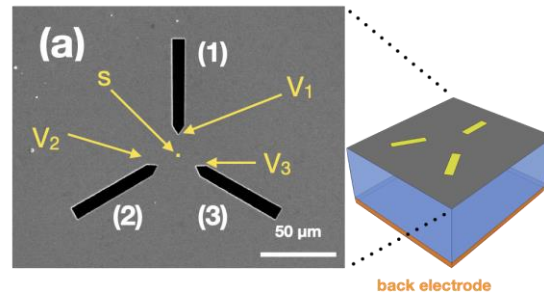


ION STRIKE POSITION AS FUNCTION OF CCE



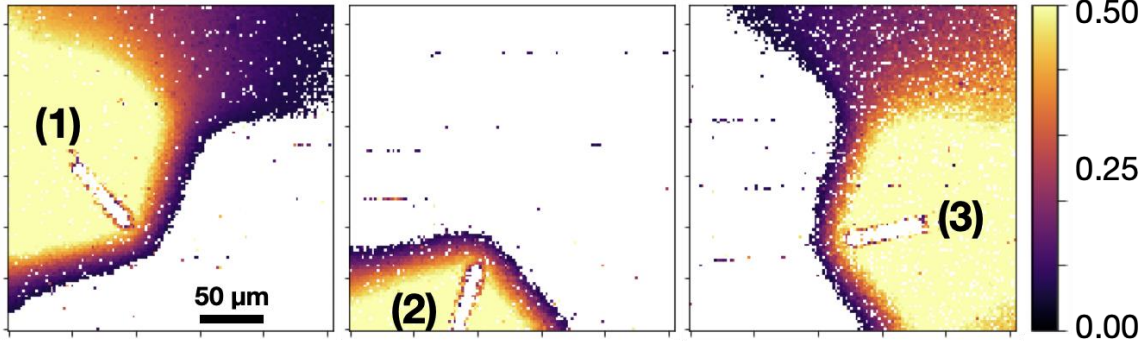
POSITION SENSITIVE DETECTOR

A two-dimensional position sensitive diamond detector based on the multi-electrode charge sharing effect

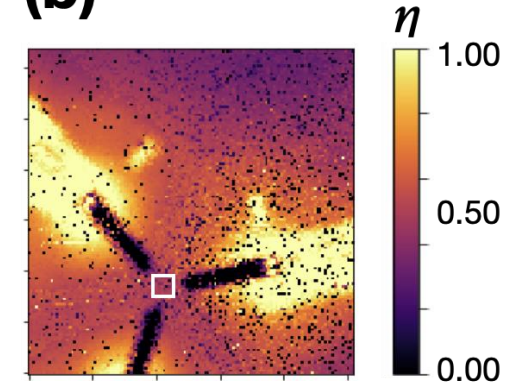


2 MeV Li

(a)

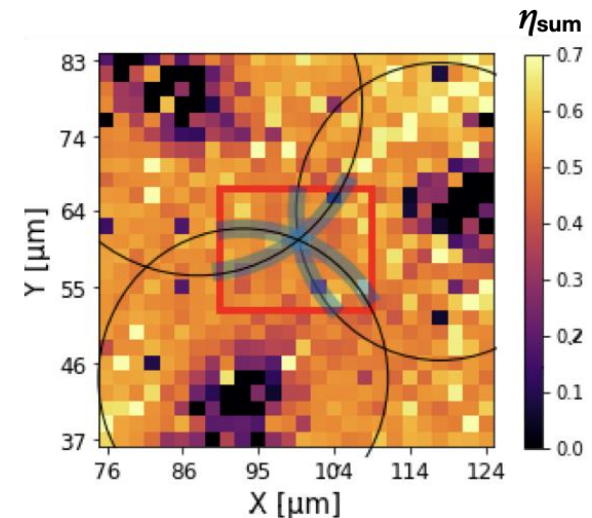


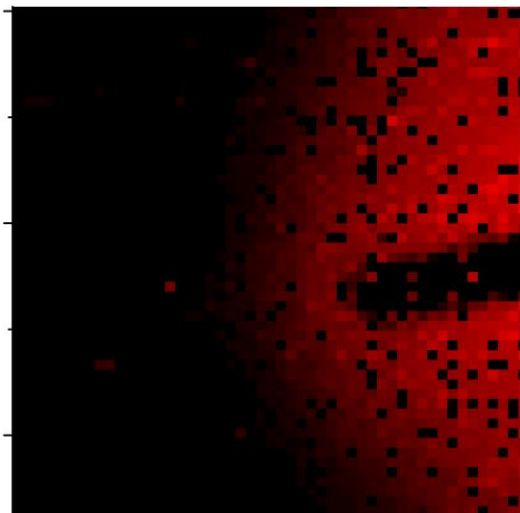
(b)



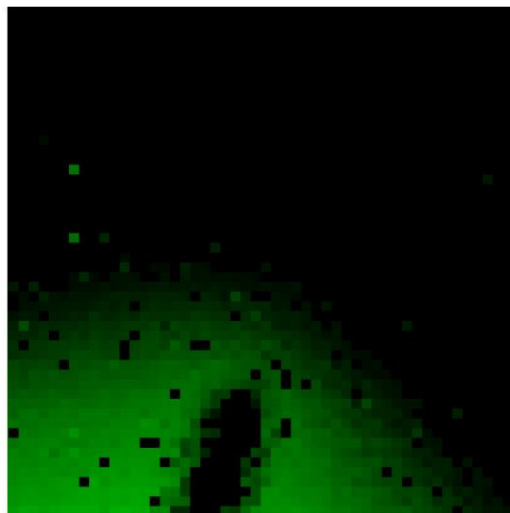
The proposed triangulation approach has demonstrated the potential to retrieve the 2-dimensional position of impact of each ion by a with a spatial uncertainty of **0.9 μm** on each spatial coordinate over a region denoted by **12 μm** length scale.

l)

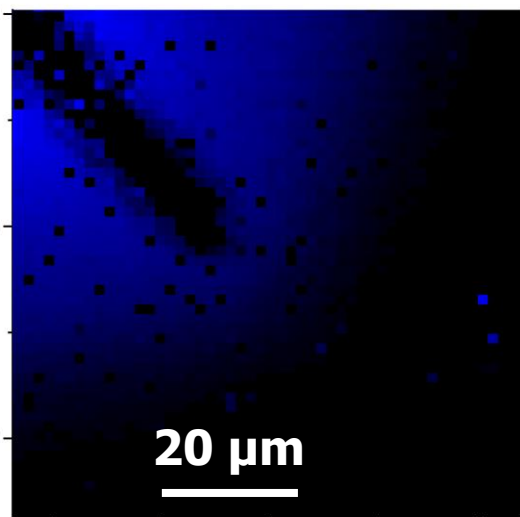
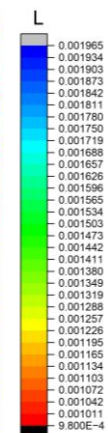
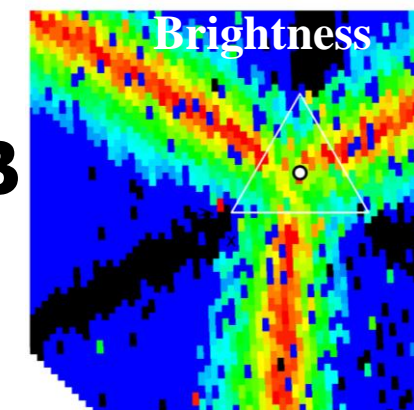
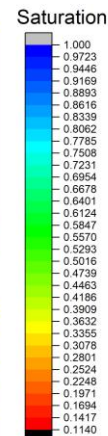
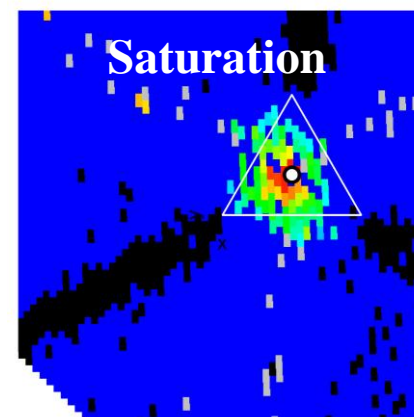




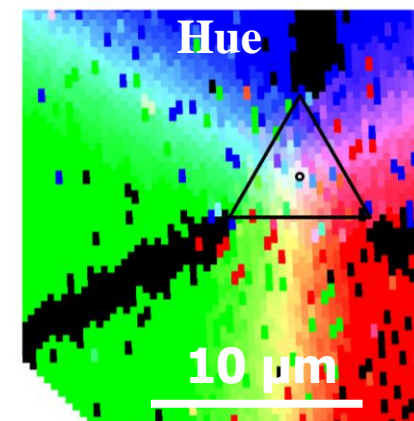
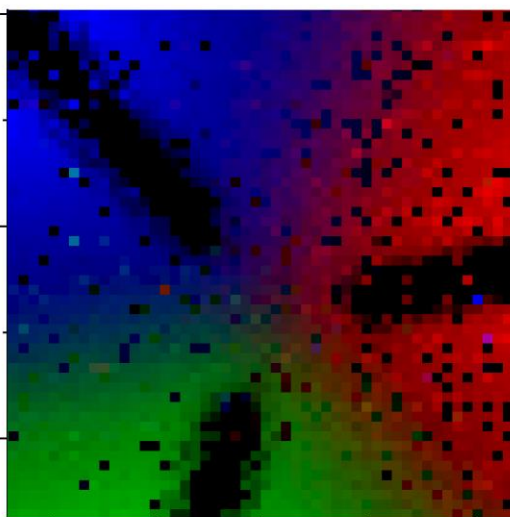
RGB



HSB



20 μm



10 μm



What next

F Tuesday, 16 January 2018

The **Italian Agency for Research Evaluation** published the list of 180 University Departments funded for excellence.

The Department of Physics of the University of Torino was ranked third best in Italy in its field and first among those whose project was submitted to peer review evaluation of the proposal.

WP

- Innovative sensors and detectors
- Dark universe and cosmic messengers
- Physics of Complex Systems

WPIa is oriented towards the development of devices and sensors based on innovative materials, which will enable the implementation of advanced methodologies in quantum technologies, biophysics, cultural heritage and (opto)electronics.

In the field of quantum technologies, a state-of-the-art multi-elemental ion implanter is going to be installed at the Solid State Physics laboratory, which will allow the multi-parametric defect engineering of wide-bandgap semiconductors (diamond, SiC, GaN, etc.) for the development of innovative single photon sources and quantum sensors. The ion implanter will operate in synergy with the recently established class 10'000 cleanroom



UNIVERSITÀ
DI TORINO



Leipzig, January-June 2018



UNIVERSITÀ DEGLI STUDI DI TORINO
Direzione Bilancio e Contratti
Area Appalti e Contratti

University of Leipzig
Ritterstraße 26
04109 Leipzig
Germany

Ref no. 195976 dated 29/05/2019

We hereby inform you that, by Executive Decree no. 2065 of 29/5/2019, your Institution has been assigned the above contract,

100 kV Implanter - University Torino

Design Document

16 December 2019

Prepared by University Leipzig



9 march 2020

Italy is in total lockdown



11 march 2020



Ettore Vittone



NIS COLLOQUIUM ITACA 12th-13th June 2023



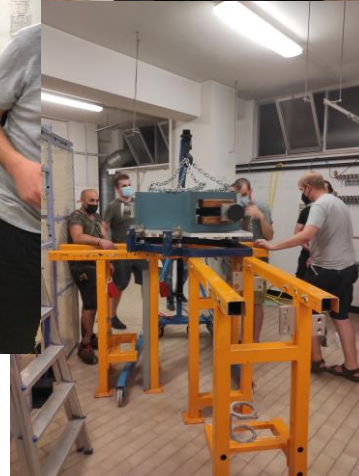
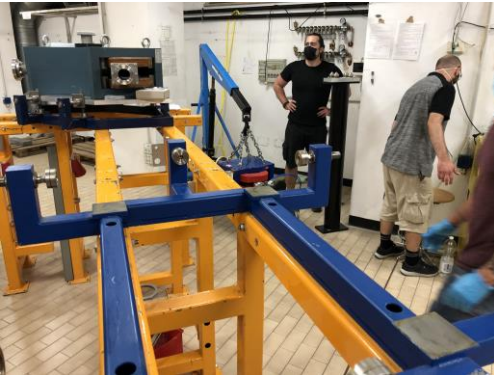


UNIVERSITÀ
DI TORINO



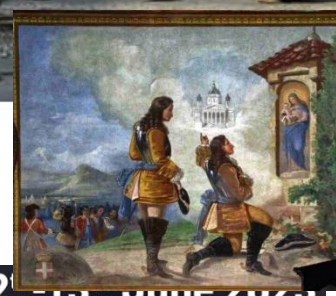
Universität Stuttgart

14 July 2021



Ettore Vittone

NIS COLLOQUIUM ITACA 12th-13th June 2023



Max terminal potential: 100 kV

Ion source: NEC – SNICS II

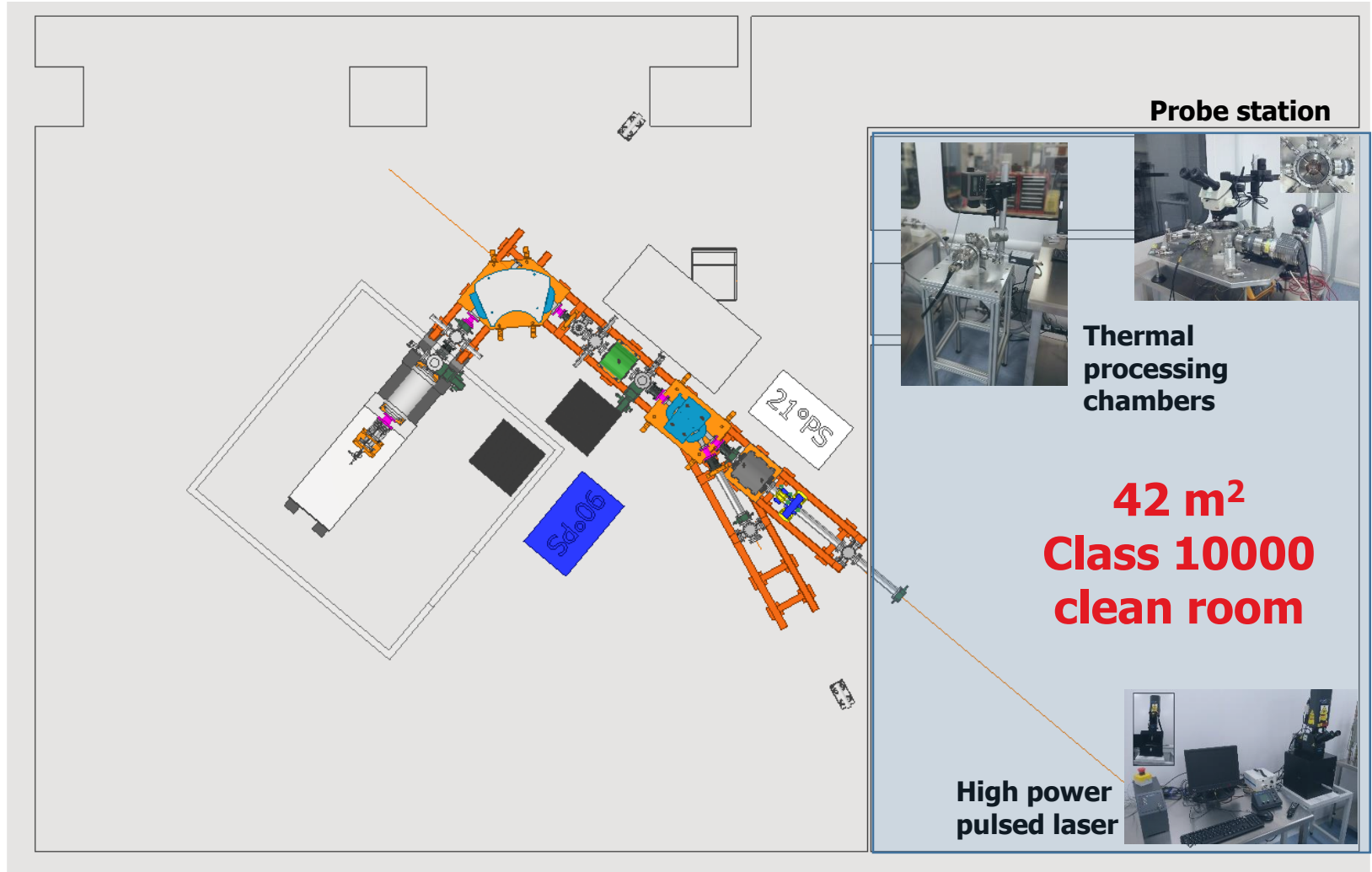
2 beamlines (one currently operational)

Typical ion beam current range: 1 pA – 1 μ A

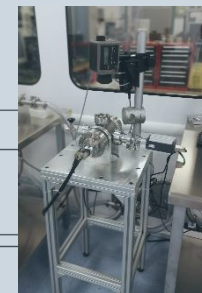
Irradiation chamber localized within the cleanroom facility



The multi-elemental ion implanter Solid State Physics Laboratory Physics Department, University of Torino



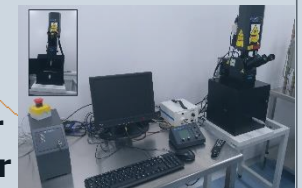
Probe station



Thermal
processing
chambers

**42 m²
Class 10000
clean room**

High power
pulsed laser



Periodic Table of the Elements

1 H Hydrogen 1.008																	2 He Helium 4.002602
3 Li Lithium 6.94	4 Be Beryllium 9.012182											5 B Boron 10.81	6 C Carbon 12.011	7 N Nitrogen 14.007	8 O Oxygen 15.999	9 F Fluorine 18.99840323	10 Ne Neon 20.1797
11 Na Sodium 22.98976928	12 Mg Magnesium 24.304											13 Al Aluminum 26.9815385	14 Si Silicon 28.0855	15 P Phosphorus 30.973761998	16 S Sulfur 32.06	17 Cl Chlorine 35.45	18 Ar Argon 39.948
19 K Potassium 39.0983	20 Ca Calcium 40.078	21 Sc Scandium 44.955908	22 Ti Titanium 47.867	23 V Vanadium 50.9415	24 Cr Chromium 51.9961	25 Mn Manganese 54.938044	26 Fe Iron 55.845	27 Co Cobalt 58.933194	28 Ni Nickel 58.6934	29 Cu Copper 63.546	30 Zn Zinc 65.38	31 Ga Gallium 69.723	32 Ge Germanium 72.630	33 As Arsenic 74.921595	34 Se Selenium 78.971	35 Br Bromine 79.904	36 Kr Krypton 83.798
37 Rb Rubidium 85.4678	38 Sr Strontium 87.62	39 Y Yttrium 88.90584	40 Zr Zirconium 91.224	41 Nb Niobium 92.90637	42 Mo Molybdenum 95.94	43 Tc Technetium (98)	44 Ru Ruthenium 101.07	45 Rh Rhodium 102.90550	46 Pd Palladium 106.42	47 Ag Silver 107.8682	48 Cd Cadmium 112.414	49 In Indium 114.818	50 Sn Tin 118.710	51 Sb Antimony 121.760	52 Te Tellurium 127.60	53 I Iodine 126.90447	54 Xe Xenon 131.294
55 Cs Cesium 132.90545196	56 Ba Barium 137.327	57 - 71 Lanthanoids	72 Hf Hafnium 178.49	73 Ta Tantalum 180.94788	74 W Tungsten 183.84	75 Re Rhenium 186.207	76 Os Osmium 190.23	77 Ir Iridium 192.222	78 Pt Platinum 195.084	79 Au Gold 196.966569	80 Hg Mercury 200.592	81 Tl Thallium 204.38	82 Pb Lead 207.2	83 Bi Bismuth 208.98040	84 Po Polonium (209)	85 At Astatine (210)	86 Rn Radon (222)
87 Fr Francium (223)	88 Ra Radium (226)	89 - 103 Actinoids	104 Rf Rutherfordium (261)	105 Db Dubnium (262)	106 Sg Seaborgium (263)	107 Bh Bohrium (264)	108 Hs Hassium (265)	109 Mt Meitnerium (266)	110 Ds Darmstadtium (268)	111 Rg Roentgenium (269)	112 Cn Copernicium (285)	113 Nh Nihonium (286)	114 Fl Flerovium (289)	115 Mc Moscovium (288)	116 Lv Livermorium (293)	117 Ts Tennessine (294)	118 Og Oganesson (294)
57 La Lanthanum 138.90547	58 Ce Cerium 140.12	59 Pr Praseodymium 140.90768	60 Nd Neodymium 144.242	61 Pm Promethium (145)	62 Sm Samarium 150.36	63 Eu Europium 151.964	64 Gd Gadolinium 157.25	65 Tb Terbium 158.92535	66 Dy Dysprosium 162.500	67 Ho Holmium 164.93033	68 Er Erbium 167.259	69 Tm Thulium 168.93402	70 Yb Ytterbium 173.045	71 Lu Lutetium 174.967			
89 Ac Actinium (227)	90 Th Thorium 232.0377	91 Pa Protactinium 231.03688	92 U Uranium 238.02891	93 Np Neptunium (237)	94 Pu Plutonium (244)	95 Am Americium (243)	96 Cm Curium (247)	97 Bk Berkelium (247)	98 Cf Californium (251)	99 Es Einsteinium (252)	100 Fm Fermium (257)	101 Md Mendelevium (258)	102 No Nobelium (259)	103 Lr Lawrencium (260)			

From 27/10/2022 to 11/05/2023
370 operating hours

Targets: diamond, Si, SiC, Ti, Metal Oxides



UNIVERSITÀ
DI TORINO



Conclusions

The Solid State Physics group of the Physics Department of the University of Torino has been committed since 90's in IBT

Main contributions

To the development of the IBIC technique for the electronic characterization of semiconductor materials and devices.

To formulate an experimental protocol, supported by a theoretical model, for the assessment of the radiation hardness of semiconductors.

To the development of new position sensitive detectors based on the sharing of the induced charge in multiple electrode systems.

To the functionalization of materials by ion beams

Acknowledgements

- The administrative staff of UniTo
 - The Department of Physics: former and current directors
 - The Radioprotection Service
 - The University of Leipzig
-
- Mr. Nunzio Dibiase

